

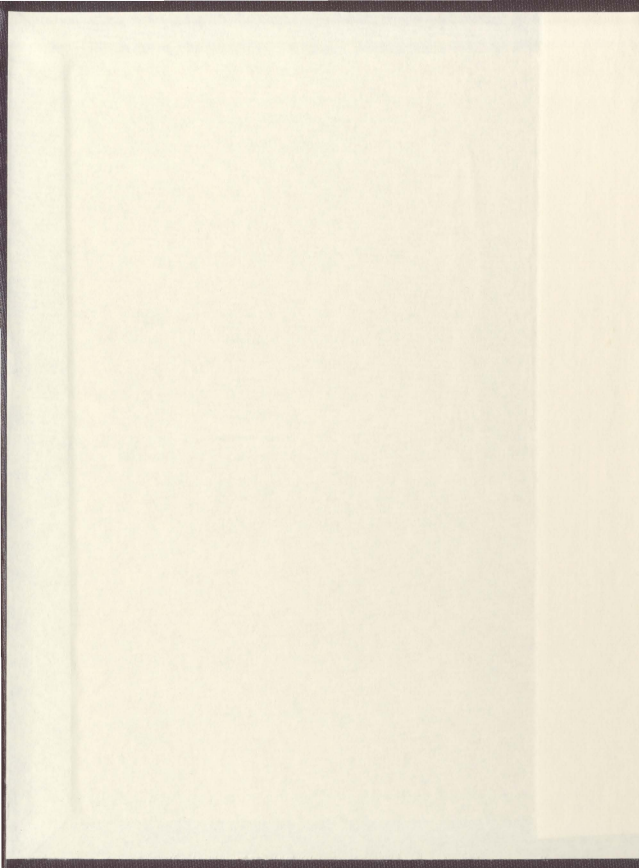
AB INITIO STUDY OF POLARIZABILITIES OF
OLIGOTHIOPHENE, OLIGOCYCLOPENTADIENE,
OLIGOFULVENE AND THEIR CYANO
SUBSTITUTED OLIGOMERS

CENTRE FOR NEWFOUNDLAND STUDIES

**TOTAL OF 10 PAGES ONLY
MAY BE XEROXED**

(Without Author's Permission)

SULTANA FERDOUS



**Ab Initio Study of Polarizabilities of
Oligothiophene, Oligocyclopentadiene,
Oligofulvene and Their Cyano
Substituted Oligomers**

By

Sultana Ferdous

A thesis submitted to the School of Graduate Studies
in partial fulfillment of the requirements for the degree of
Master of Science



Department of Physics and Physical Oceanography
Memorial University of Newfoundland

08 September 2004

St. John's

Newfoundland

ABSTRACT

Ab Initio study of polarizabilities and first order hyperpolarizabilities of thiophene, fulvene and cyclopentadiene based conducting oligomers and polymers and their cyano derivatives have been performed using the Hartree-Fock (HF), configuration interaction singles (CIS) and density functional (DFT) theories with 3-21G* basis using Gaussian 94, 98 and 03 softwares. The main motivation for this investigation is to determine the correlation between the excitation energies and polarizabilities and hyperpolarizabilities for the conjugated systems studied. It has been found that HF and DFT approaches give similar magnitudes for polarizabilities whereas CIS theory provides results that are considerably different. All three methods predict similar trends in polarizabilities as a function of oligomer length and bond alternation along the backbone of the oligomers. It has also been observed that the end groups and the number of 'double' bonds have a significant effect on the magnitude of polarizability per C-C bond. Comparison with experimental results has been made where possible.

ACKNOWLEDGMENT

I would like to thank my supervisor Dr. Jolanta B. Lagowski for her guidance, support, encouragement and valuable suggestions throughout the whole research work.

I am grateful and wish to thank to my parents, without their love, support and guidance I would not be where I am today. This thesis is dedicated them.

I would like to thank Memorial University of Newfoundland for awarding Graduate Scholarship and the Department of Physics and Physical Oceanography for offering me Teaching Assistantship.

I would like to thank National Science and Engineering Research Council of Canada (NSERC) for their partial financial support.

I also wish to thank to Advanced Computation Visualization Centre (CVC) for computational resources.

I am thankful to the system administrator of the department Mr. Fred Perry and John Jerrett for their sincere cooperation and computational support. My special thanks go to the graduate student Muzaddid Sarker for his warm cooperation.

CONTENTS

Table of Contents	iii
List of Figures	vi
List of Tables	x
1. INTRODUCTION	1
1.1 Conducting polymers	1
1.2 Literature review	7
1.3 Current research work	13
2. THEORETICAL APPROACH	17
2.1 General approach	17
2.2 The electronic Hamiltonian of a system	20
2.3 Hartree-Fock theory	21
2.3.1 HF equations	22
2.3.2 Basis set expansions of HF wave functions	24
2.4 Configuration interaction singles	25
2.4.1 CIS wave functions	26
2.5 Density functional theory	28
2.5.1 KS formalism	30
2.6 Energy derivatives formulation	31
2.7 Sum over states	33

3. COMPUTATIONAL APPROACH	38
3.1 Computational details	38
4. POLARIZABILITY VS CHAIN LENGTH	43
4.1 Polarizability vs the monomer length - infinite chain length limit	43
4.2 Polarizability per monomer vs oligomer length	48
4.3 Polarizability and excitation energy	51
5. POLARIZABILITY VS BOND LENGTH ALTERNATION	54
5.1 OLIGOACETYLENE (OA)	55
5.1.1 Average polarizability per C-C bond vs bond length alternation	56
5.1.2 First order hyperpolarizability vs bond length alternation	58
5.1.3 Excitation energy vs bond length alternation	60
5.2 OLIGOTHIOPHENE (OTH)	61
5.2.1 Average polarizability per C-C bond vs bond length alternation	61
5.2.2 First order hyperpolarizability vs bond length alternation	63
5.2.3 Excitation energy vs bond length alternation	65
5.3 OLIGOCYCLOPENTADIENE (OCY)	66
5.3.1 Average polarizability per C-C bond vs bond length alternation	66
5.3.2 First order hyperpolarizability vs bond length alternation	68
5.3.3 Excitation energy vs bond length alternation	69
5.4 OLIGOFULVENE (OFV)	70

5.4.1 Average polarizability per C-C bond vs bond length alternation	70
5.4.2 First order hyperpolarizability vs bond length alternation	72
5.4.3 Excitation energy vs bond length alternation	74
5.5 OLIGO-DICYANOMETHYLENE CYCLO- - PENTADITHIOPHENE (OCNTH)	75
5.5.1 Average polarizability per C-C bond vs bond length alternation	75
5.5.2 First order hyperpolarizability vs bond length alternation	77
5.5.3 Excitation energy vs bond length alternation	79
6. DISCUSSIONS AND CONCLUSIONS	81
6.1 Comparison of OTH, OCY and OFV	82
6.2 Comparison of OCNTH, OCNCY and OCNFV	85
6.3 Comparison of OTH and OCNTH	86
6.4 Comparison of our results with the previous works	90
6.5 Conclusions	94
6.6 Future work	101
7. BIBLIOGRAPHY	102
8. APPENDIX	113
SUPPLEMENTARY DATA	113

LIST OF FIGURES

1.1	Monomers of the π conjugated systems studied.	14
1.2	Monomers of aromatic and quinonoid forms of OTH.	15
4.1	(a) Approximate average and (b) average polarizability as function of the inverse of the oligomer length in SOS method.	44
4.2	(a) Polarizability as a function of the inverse of the oligomer length in CIS method.	46
4.2	(b) $\ln(\text{average polarizability})$ as a function of the $\ln(\text{oligomer length})$ in CIS method.	46
4.3	(a) Approximate average and (b) average polarizability per monomer as a function of the oligomer length in SOS method.	49
4.4	Average polarizability per monomer as a function of the oligomer length in CIS method.	50
4.5	Excitation energy as a function of the oligomer length in CIS method.	52
4.6	Excitation energy as a function of the polarizability per monomer in CIS method.	53
5.1	OA with 7 and 9 bonds respectively.	55
5.2	Evolution of average polarizability per C-C bond as a function of the bond length alternation for 7 ($\text{BLA} \leq 0$) and 9 ($\text{BLA} > 0$) C-C bonds of OA.	57

- 5.3 Evolution of first order hyperpolarizability (a) β_{xxx} and (b) β_{zzz} as a function of the bond length alternation for 7 (BLA \leq 0) and 9 (BLA $>$ 0) C-C bonds of OA. 59
- 5.4 Excitation energy as a function of the bond length alternation for 7 (BLA \leq 0) and 9 (BLA $>$ 0) C-C bonds of OA. 61
- 5.5 Evolution of average polarizability per C-C bond as a function of the bond length alternation for the aromatic (BLA \leq 0) and quinonoid (BLA $>$ 0) structures of OTH. 62
- 5.6 Evolution of hyperpolarizability (a) β_{xxx} and (b) β_{zzz} as a function of the bond length alternation for the aromatic (BLA \leq 0) and quinonoid (BLA $>$ 0) structures of OTH. 64
- 5.7 Excitation energy as a function of the bond length alternation for the aromatic (BLA \leq 0) and quinonoid (BLA $>$ 0) structures of OTH. 66
- 5.8 Evolution of average polarizability per C-C bond as a function of the bond length alternation for the aromatic (BLA \leq 0) and quinonoid (BLA $>$ 0) structures of OCY. 67
- 5.9 Evolution of first order hyperpolarizability β_{zzz} as a function of the bond length alternation for the aromatic (BLA \leq 0) and quinonoid (BLA $>$ 0) structures of OCY. 68
- 5.10 Excitation energy as a function of the bond length alternation for the aromatic (BLA \leq 0) and quinonoid (BLA $>$ 0) structures of OCY. 70

- 5.11 Evolution of average polarizability per C-C bond as a function of the bond length alternation for the aromatic ($BLA \leq 0$) and quinonoid ($BLA > 0$) structures of OFV. 71
- 5.12 Evolution of first order hyperpolarizability (a) β_{xxx} and (b) β_{zzz} as a function of the bond length alternation for the aromatic ($BLA \leq 0$) and quinonoid ($BLA > 0$) structures of OFV. 73
- 5.13 Excitation energy as a function of the bond length alternation for the aromatic ($BLA \leq 0$) and quinonoid ($BLA > 0$) structures of OFV. 75
- 5.14 Evolution of average polarizability per C-C bond as a function of the bond length alternation for the aromatic ($BLA \leq 0$) and quinonoid ($BLA > 0$) structures of OCNTH. 76
- 5.15 Evolution of first order hyperpolarizability (a) β_{xxx} and (b) β_{zzz} as a function of the bond length alternation for the aromatic ($BLA \leq 0$) and quinonoid ($BLA > 0$) structures of OCNTH. 78
- 5.16 Excitation energy as a function of the bond length alternation for the aromatic ($BLA \leq 0$) and quinonoid ($BLA > 0$) structures of OCNTH. 79
- 6.1 Evolution of excitation energy as a function of average polarizability per monomer of the dimer molecules in (a) HF, (b) CIS and (c) DFT methods. 83
- 6.2 Evolution of average polarizability per C-C bond as a function of bond length alternation for the aromatic ($BLA \leq 0$) and quinonoid ($BLA > 0$) structures of OTH and OCNTH in (a) HF, (b) CIS and (c) DFT methods. 87

- 6.3 Evolution of the first order hyperpolarizability as a function of bond length alternation for the aromatic ($BLA \leq 0$) and quinonoid ($BLA > 0$) structures of OTH and OCNTH in (a) HF and (b) DFT methods. 88
- 6.4 Evolution of excitation energy as a function of bond length alternation for the aromatic ($BLA \leq 0$) and quinonoid ($BLA > 0$) structures of OTH and OCNTH in (a) HF, (b) CIS and (c) DFT methods. 89

LIST OF TABLES

- | | | |
|-----|---------------------------------------------------------------------------------------------------------------------------------------------------------------------------------------------------|----|
| 6.1 | Comparison of our calculated data and the experimental data of α/n for OTH. | 90 |
| 6.2 | Comparison of our calculated CIS excitation energies (in eV) with Chakraborty <i>et al.</i> for different oligomer with the method/basis set RCIS/3-21G*. | 92 |
| 6.3 | Comparison of our calculated CIS excitation energies (in eV) with Chakraborty <i>et al.</i> for the different oligomers in their most stable configuration with the method/basis set RCIS/3-21G*. | 93 |

Chapter 1

INTRODUCTION

1.1 Conducting polymers

Conducting polymers are conjugated polymers, in particular organic compounds that have an extended π -orbital system, through which electrons can move from one end of the polymer to the other [1]. The most important aspects of conjugated polymers are their ability to act as electronic conductors and to exhibit nonlinear optical (NLO) properties. The basic structural characteristic of all conjugated polymers is their quasi-infinite π system extending over a large number of recurring monomer units. This characteristic results in materials with directional conductivity, strongest along the axis of the chain. The mechanism of conductivity in these polymers is based on the motion of charged defects within the conjugated framework. The conjugated polymers are semiconductors or insulators in their neutral state. They can be made conductive by oxidation (p-doping) or reduction (n-doping) of the polymer either by chemical or electrochemical means, generating the mobile charge carriers [1].

Charge carriers, either positive p-type (holes) or negative n-type (electrons), give rise to conductivity. The conductivity σ of a conducting polymer is related to the number of charge carriers, n , and their mobility, μ , that is, $\sigma \propto n \mu$ [2].

The physical and chemical properties of organic polymers, especially heterocyclic conjugated systems, have attracted much interest both experimentally and theoretically in recent years [3]. At present, scientists are also interested in the σ -conjugated polysilane polymers which have a number of physical properties such as transparency in the visible region of the spectrum, thermal and oxidative stability, high resolution imageability etc. [4].

Conducting organic polymers have received extensive interest since the highlight reports of remarkable increase in conductivity upon halogen doping of polyacetylene by Shirakawa *et al.*, Heeger and MacDiarmid [5]. Since these discoveries, many experimental and theoretical studies have been performed both on short chain conjugated oligomers and on the full polymers. Conducting polymers have the qualities to combine the high conductivity of pure metals with the processibility, corrosion resistance and low density of polymers. They are very useful in the applications of electrochromic displays, electromagnetic shielding, sensor technology, non-linear optics, molecular electronics, conducting fabrics, antistatic coatings for use in photographic films or electronic device fabrication and low-voltage electrochromic windows to organic light emitting diodes, photodiodes, and photovoltaic devices [5, 6].

In recent years, many experimental and theoretical works have focused on the design of new π -conjugated polymers with very small band gap ($E_g < 1\text{eV}$). These polymers even in their intrinsic ground states show conductive or at least semiconductive properties. For designing new kinds of polymers, it is important to understand the evolution of the band gaps of conjugated polymers with respect to their chemical structures. A large number of theoretical studies have been done in the recent years to understand the relationship between the chemical and electronic structures of conjugated polymers [7]. This coupling of chemical and electronic structure is the source of much of the fascinating physics of π -conjugated oligomers [8].

Polyacetylene has the simplest conjugated structure. Because of its degenerate ground state of the all-trans-isomer, it allows the existence of mobile neutral spin defects (solitons), whose behavior is of great interest to solid-state physicists [9]. Conjugated organic polymers have attracted a lot of attention ever since the discovery of the very high electrical conductivity of polyacetylene upon doping. Their conductivities in doped states are of the order of, or larger than, that of copper at room temperature (as in the case of recently reported iodine-doped polyacetylene). Examples of other important conjugated polymers are polyparaphenylene, polypyrrole, polyaniline, polythiophene, and their derivatives. Similar to polyacetylene, when they are oxidized or reduced, they exhibit transitions from the insulating or semiconducting state to the highly conducting regime [10]. In addition to their conductivity properties, organic compounds with delocalized π -electron systems are leading candidates for NLO materials.

The knowledge of the polarizabilities and hyperpolarizabilities is required for the designing of optimized materials for photonic devices such as electro-optic modulators and optical switches [11]. For example, the novel π -conjugated polymer, polydiethynylsilane (PDES) has excellent nonlinear optical properties. This new material is easily processed, soluble in a variety of solvents and stable in air. The structures of several forms of PDES have been characterized theoretically by Grigoras *et al.* [12]. The NLO properties are being increasingly exploited in a variety of optoelectronic and photonic applications. For example, the third-order nonlinear optical phenomenon of an optically-induced change in refractive index is fundamental to all-optical switching and computing, as well as phase conjugate adaptive optics [13].

Worldwide, scientists are doing research on materials which exhibit linear and nonlinear activities [14]. It is true that both linear and nonlinear responses are very important for both scientific and technological applications. These days, however, nonlinear electric responses receive much of the interest due to their contributions in telecommunications. In summary, in the recent years, the electrical conductivities and nonlinear optical responses of conjugated polymers have attracted enormous attention among theorists and experimentalists [15].

The optimization of materials for NLO devices first requires an in-depth understanding of the NLO properties at the microscopic, or molecular level. The properties such as polarizabilities (α), hyperpolarizabilities (β , γ , ...) are required for the rational design of the optimized materials for

photonic devices such as electro-optic modulators, all-optical switches etc. The NLO properties of the conjugated molecules and polymers are very responsive to the variations in chemical structure, conjugation length, donor and acceptor substitutions and the presence of defects or dopants [16]. The NLO properties of conjugated polymers may have exceptionally large values due to conjugation and the factors mentioned above [17].

Bond length alternation (BLA) is defined as the difference between 'single' and 'double' adjacent bonds along the chain backbone (see Chapter 3). The magnitude of the BLA along the backbone of a conjugated system is recognized as a crucial parameter for tuning its electronic properties [18]. It is also a key parameter used in optimizing the linear and NLO properties of organic conjugated compounds [15, 18]. In order to design low-band-gap polymers as well as new active species in light-emitting diodes, the BLA of conjugated polymers and oligomers has been varied by chemical modifications. BLA also plays a substantial role in the conductivity phenomenon of doped organic conjugated polymers [18].

Because of their potential role in optical communication devices, the nonlinear polarizabilities i.e., hyperpolarizabilities, have received significant attention. The first order hyperpolarizability (see Chapter 2) is related to the macroscopic NLO phenomena i.e., second harmonic generation, optical rectification etc. In order to maximize the hyperpolarizability per unit cell, the electron delocalization, asymmetry and the length or weight of the compound have to be efficiently combined [19]. For the organic systems, the first order hyperpolarizability increases by the presence of the mobile π electrons and it is zero for centro-symmetric molecules as it

corresponds to an odd term in the dipole moment Taylor series expansion [19].

To observe the nonlinear effects, a lot of the research works have been carried out, mostly on oligothiophenes (OTH). This is mainly for two reasons; firstly, this material is stable under normal conditions and very flexible with respect to modifications of its chemical structure and secondly, it is a very promising candidate due to its high nonlinear optical properties. It can be used in a wide range of applications from optoelectronics to information-storage devices [3].

It is often constructive to carry out experiments on shorter-length, well-defined oligomers as the exact length distributions and geometries of long-length conducting polymers are frequently not well characterized. This circumvents many experimental difficulties coming up from the poor solubility and processability of many of the full length polymers, although some physical measurements have been carried out on thin-film samples [5].

1.2 Literature review

Organic molecules with conjugated π chains have large dipole polarizabilities and hyperpolarizabilities which increase rapidly with chain length. A reliable understanding of the dependence of these properties on the molecular structure requires exact calculations for some short-chain molecules [20]. In recent years, the focus on the *ab initio* calculation of polarizabilities and hyperpolarizabilities has increased tremendously and hence it is easier to provide a theoretical basis for analyzing molecular electrical interactions [21]. For the conjugated systems the lowest (singlet) excited state often corresponds to a transition from the highest occupied π molecular orbital (HOMO) to the lowest unoccupied π^* molecular orbital (LUMO) levels. It is found by Chakraborty *et al.* that with the increase of the chain length the excitation energies have red shifted [22]. In order to put our work in the appropriate framework, we have reviewed previous related works.

The static polarizabilities and the hyperpolarizabilities for the ground states of the linear polyynes 1,3-butadiyne (C_4H_2); 1,3,5-hexatriyne (C_6H_2) and 1,3,5,7-octatetrayne (C_8H_2) have been calculated by finite-field methods by Maroulis *et al.* [20]. This was the first dependable *ab initio* determination of the increase of those properties with the chain length. C_4H_2 , C_6H_2 and C_8H_2 are polyynes that are similar to studied compounds, however instead of double and single bonds there are alternating triple and single bonds along the chain backbone. Maroulis *et al.*, in their investigation on linear $C_{2n}H_2$ polyynes, found that with the increase of the chain length, n , the

longitudinal component of the polarizability increases linearly as $n^{1.5}$ and the mean polarizabilities increase as $n^{1.2}$ [20]. Edet *et al.* also studied the chain length dependence of static longitudinal polarizabilities using *ab initio* calculations in linear $C_{2n}H_2$ polyynes [23]. They found that the growth of the response properties with n slow down with the increase of the chain length. For large n , α grows linearly with n . Dalskov *et al.* carried out a study on the polyene series, $C_{2n}H_2$, to calculate the static longitudinal polarizabilities using both the uncorrelated random phase approximation and the correlated second-order polarization propagator approximation [24]. The static longitudinal polarizability of the C_4H_2 through $C_{54}H_2$ polyene was studied at the HF level of theory by Toto *et al.* [25].

Chopra *et al.* have computed the static polarizabilities of polyenes by *ab initio* SCF theory with the basis sets STO-3G and 3-21G and have shown that the longitudinal polarizability increases as $n^{1.36}$ and $n^{1.44}$ respectively for short chains [26]. They have noticed that the growth of the longitudinal component of α is the largest among the diagonal components of polarizability. It has been observed from the previous calculation that the electron correlation plays only a minor role in the dipole polarizabilities and hyperpolarizabilities. With the increase of the chain length, the intramolecular polarization becomes relatively more important and fewer basis sets are required for the calculation of longitudinal polarizabilities [26, 27]. It has been found by Hurst *et al.* that the basis set requirements diminish with increasing chain length in the polyenes [27].

The static dipole polarizability for the polyene systems via *ab initio* coupled-perturbed Hartree-Fock (HF) theory was studied by Hurst *et al.* [27]. They

found that the longitudinal component of the polarizability increases with the increase of the chain length. For the shorter polyenes the longitudinal component of the polarizability $\propto n^{1.6}$ but for larger n , they obtained a linear relationship. They also noticed that the longitudinal component is the largest which is consistent with the fact that a strong response of the delocalized π electrons to the electric fields is along the chain backbone.

Benoît *et al.* have computed the static electronic longitudinal polarizability of all-trans planar polyacetylene chains with restricted Hartree-Fock (RHF), second-order Møller-Plesset (MR2) and the density functional schemes based on the SVWN and B3LYP exchange correlation functionals by varying the bond length alternation along the conjugated backbone [18]. The four methods show that α decreases with the increase of BLA from 0.005Å to 0.225Å i.e., the smaller the BLA, the larger the α would be. They found that the BLA dependence of α in RHF is overestimated by a factor of 2-3 with respect to the MP2 procedure [18]. Using sum-over-states (SOS) perturbation theory π electron polarizabilities of finite and infinite organic polymers i.e., polyacetylene and various polyheterocycle have been calculated by Ducasse *et al.* [28].

π -electron calculations of the polarizabilities in conjugated systems (polyenes) with the finite-field technique have been investigated by Villesuzanne *et al.* [29]. They found that in neutral systems, the polarizability per monomeric unit increases smoothly and then shows an asymptotic behavior with n . But for the polymers with defects, the polarizability per monomeric unit first increases with n , reaches a

maximum polarizability per monomeric unit for large value of n and finally shows an asymptotic behavior [29].

By using the perturbative density matrix treatment de Melo *et al.* have investigated the behavior of the polarizabilities [30] and the first hyperpolarizabilities of the linear conjugated chains C_nH_{n+2} described by a Pariser-Parr-Pople Hamiltonian [31]. They observe that the polarizabilities of polyenic chains depend on the conformation and charge state of the system. The first order hyperpolarizability tensor $\overset{\equiv}{\beta}_{ijk}$ vanishes for regular polyenes and polaron chains. The three components β_{xxx} , β_{yyy} and β_{zzz} of the molecules belonging to the C_{2v} group can be nonzero. De Melo *et al.* found all the components of the first order hyperpolarizability are negligible for the neutral soliton chains but the first order hyperpolarizability can be large and should increase with chain length for the charged solitons [31].

Ab initio coupled and uncoupled Hartree-Fock polarizabilities were computed for increasingly large oligothiophenes by Champagne *et al* using 3-21G, 6-31G* and Sadljej medium size polarized atomic basis sets . They found that polythiophene is more polarizable than polydiacetylene and polyyne but less polarizable than polyacetylene [15].

Meyers *et al.* studied the influence of an external, static electric field on the linear and nonlinear polarizabilities of a set of π -electron chromophores [32]. In the 9-(dimethylamino)nona-2,4,6,8-tetraenal molecule (DAO), they found that the polarizabilities are totally dominated by the longitudinal

tensor components and maximum at the cyanine limit (BLA=0). But with the increase of bond order alternation (BOA), the first order hyperpolarizability increases first, peaks in a positive sense, then decreases and passes through zero at the cyanine limit, and then becomes negative and peaks in a negative sense and then decreases again. It was noted by them that the shape of the first order hyperpolarizability versus BOA is the first order derivative-like with respect to the α evolution [32].

Luo *et al.* investigated the solvent effects on the static polarizabilities and hyperpolarizabilities of the conjugated polymers using a semiclassical solvation model using results from *ab initio* calculations [33]. *Ab initio* coupled HF investigation of the static first order hyperpolarizability of model all-trans-polymethineimine oligomers (conjugated chains made of alternating carbon and nitrogen atoms) has been studied by Champagne *et al.* [34].

Grozema *et al.* have studied the excited state polarizabilities of conjugated molecules using time dependent density functional theory [35]. *Ab initio* HF and density functional theory (DFT) studies of the static dipole polarizabilities and first order hyperpolarizabilities of fulvene monomer have been carried out by Hinchliffe *et al.* [36]. Jacquemin *et al.* studied the longitudinal electronic first order hyperpolarizability of carbon-silicon analogues to polyacetylene using *ab initio* method taking into account dynamic electron correlation effects [19].

Few experimental studies of polarizabilities and hyperpolarizabilities of conjugated oligomers or polymers have been performed. Thienpont *et al.*

have reported the observation of saturation with the chain length of the band gap, polarizability and the first order hyperpolarizability for oligothiophenes. In their investigation, the length dependence of α is given by a power law and the exponent is 2.4. They found a strong length dependence of α for $n \leq 7$ and that become weaker, more or less linear for $n > 7$, where the band gap becomes constant, i.e., the saturation occurs at about seven repeat units [37]. Zhao *et al.* carried out a systematic study on the thiophene series from monomer to hexamer to find out the dependence of the band gap and the polarizability on the number of repeat unit [38]. The averaged polarizabilities are measured from the refractive index measurements of THF solutions.

With regard to the excitation energies, Chakraborty and Lagowski [22, 39] carried out an extensive study to determine the nature of the geometric conformations and electronic transitions in π -conjugated OTH and their cyano derivatives, and also oligocyclopentadiene (OCY) and oligofulvene (OFV) and their cyano derivatives. They observed trends in excitation energies of these systems as a function of the chain lengths by using the singles configuration interaction (CIS) theoretical approach. The study on thiophene and cyclopentadiene-based polymers by using semi-empirical molecular orbital theory (MNDO, AM1) followed by *ab initio* HF method was done by Subramanian and Lagowski [40].

Using the time-dependent density functional theory with B3LYP functional, Jing *et al.* carried out a study on polyacetylene, polycyclopentadiene and polythiophene to find out the chain length dependence on the excitation energies of these oligomers [41]. The energy band gap of

thiophene (monomer and dimer) was investigated using both *ab initio* molecular orbital quantum theory and DFT methods by Arnold *et al.* The calculations were carried out initially at the HF level of theory [6].

1.3 Current research work

The main goal of this present work is to investigate the polarizabilities and hyperpolarizabilities of conducting polymers by using *ab initio* methods. Monomeric units of the studied systems are shown in figure 1.1. We have divided our investigation into two parts. In the first part, *ab initio* calculations of polarizabilities have been carried out on oligomers (ranging from 1 to 16 monomers long) OTH, OCY, OFV, oligo-(dicyanomethylene cyclopentadithiophene) (OCNTH), oligo-(dicyano-methylene cyclopentadiene) (OCNCY) and oligo-(dicyanomethylene cyclopentadi-fulvene) (OCNFV) with SOS and CIS methods.

We have investigated the chain length dependence of the polarizabilities (α) and excitation energies (ΔE). The geometrical parameters of the oligomers have been fully optimized with the 3-21G* split valence basis set by using the GAUSSIAN 94 and GAUSSIAN 98 programs [42, 43]. We have used -H or -H₂ as the end groups in the various oligomers. It has been observed that the effect of the end group decreases as the chain length increases [15, 44].

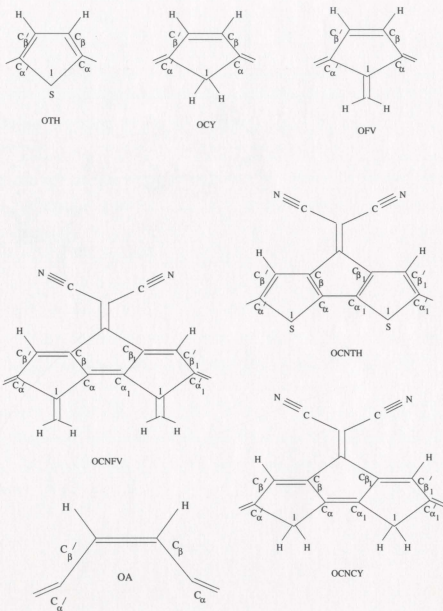


Figure 1.1: Monomers of the π conjugated systems studied.

In the second part, partial geometry optimizations on oligomers oligoacetylene (OA), OTH, OCY, OFV and OCNTH have been performed by using RHF, CIS and DFT to see the effect of BLA on α , β and ΔE . For OA, we have considered two oligomers with 7 bonds and 9 bonds; and for OTH, OCY, OFV and OCNTH, we considered unit cells consisting of two rings or dimers. We use -H as end groups for the aromatic isomer and $=H_2$ or $=CH_2$ as end groups for the quinonoid isomer. As an example of the structural forms, the aromatic and quinonoid isomers for OTH are shown in figure 1.2.

From the various investigations, it was determined that the structure of cyclopentadiene and fulvene and their cyano derivatives have greater stability in the quinonoid forms [22 and the references therein] and

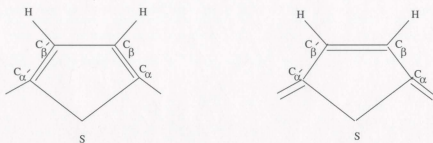


Figure 1.2: Monomers of aromatic and quinonoid forms of OTH

thiophene and its cyano derivative have greater stability in their aromatic forms. Hence we have chosen the aromatic forms for OTH and OCNTH and the quinonoid forms for OCY, OCNCY, OFV and OCNFV in the

first part of this thesis. The main reason for studying cyano substituted thiophene, cyclopentadiene and fulvene is that previous investigations [22] showed that there is a significant lowering of band gaps in these cyano derivatives in comparison to their parent oligomers. In order to gain further understanding of these compounds an investigation of their polarizabilities and hyperpolarizabilities was performed in this thesis.

In chapter 2 of this thesis, we discuss the theoretical methods used for computations. In particular we discuss HF, CIS and DFT theory in the section 2.3, 2.4 and 2.5 respectively. In chapter 3, we discuss the computational approach used for the systems studied. In chapter 4, we describe the dependence of the polarizabilities and excitation energies on the chain length for OTH, OCY, OFV, OCNTH, OCNCY and OCNFV oligomers. In chapter 5, we discuss the BLA effects upon the polarizabilities, hyperpolarizabilities and the excitation energies for OA, OTH, OCY and OCNTH. In chapter 6 we discuss the results obtained for the parent oligomers and their cyano derivatives, and compare our results with the previous works where possible. At the end we have summarize the conclusions.

Chapter 2

THEORETICAL APPROACH

2.1 General approach

When a particle is exposed to an electric field, there is a change in the charge redistribution which is characterized by a set of constants called polarizabilities [45]. The energy caused by a small uniform electric field perturbation $\vec{\mathcal{E}}$ can be written as [46]

$$H' = -\vec{\mu} \cdot \vec{\mathcal{E}} \quad (2.1)$$

where $\vec{\mu}$ is the dipole moment and is defined by

$$\vec{\mu} = \sum_i q_i \vec{r}_i \quad (2.2)$$

where q_i is the charge at the position \vec{r}_i . The Feynman-Hellmann (FH) theorem states how the energy of a system varies when the system is characterized by a Hamiltonian that depends on the perturbation parameter P [47].

In our case P is $\vec{\epsilon}$. We have assumed that $|\vec{\epsilon}|$ is very small†. By using the FH theorem and equation (2.1), we can write

$$\frac{dE}{d\vec{\epsilon}} = \left\langle \frac{\partial H}{\partial \vec{\epsilon}} \right\rangle = -\langle \vec{\mu} \rangle. \quad (2.3)$$

Since $|\vec{\epsilon}|$ is small, we can Taylor expand the energy E about $E(0) = E(\vec{\epsilon}=0)$

$$E = E(0) + \left(\frac{dE}{d\vec{\epsilon}} \right)_{\vec{\epsilon}=0} \cdot \vec{\epsilon} + \frac{1}{2!} \left(\frac{d^2 E}{d\vec{\epsilon}^2} \right)_{\vec{\epsilon}=0} \cdot \vec{\epsilon}^2 + \frac{1}{3!} \left(\frac{d^3 E}{d\vec{\epsilon}^3} \right)_{\vec{\epsilon}=0} \cdot \vec{\epsilon}^3 + \dots \quad (2.4)$$

From equations (2.3) and (2.4), the dipole moment $\vec{\mu}$ of the system can be written as [49]

$$\langle \vec{\mu} \rangle = - \left(\frac{dE}{d\vec{\epsilon}} \right)_{\vec{\epsilon}=0} - \left(\frac{d^2 E}{d\vec{\epsilon}^2} \right)_{\vec{\epsilon}=0} \cdot \vec{\epsilon} - \frac{1}{2} \left(\frac{d^3 E}{d\vec{\epsilon}^3} \right)_{\vec{\epsilon}=0} \cdot \vec{\epsilon}^2 - \frac{1}{6} \left(\frac{d^4 E}{d\vec{\epsilon}^4} \right)_{\vec{\epsilon}=0} \cdot \vec{\epsilon}^3 - \dots$$

or

$$\vec{\mu} = \vec{\mu}_0 + \vec{\alpha} \cdot \vec{\epsilon} + \frac{1}{2} \vec{\beta} \cdot \vec{\epsilon}^2 + \frac{1}{6} \vec{\gamma} \cdot \vec{\epsilon}^3 + \dots \quad (2.5)$$

The term $\vec{\mu}_0$ represents the permanent dipole moment and $\vec{\alpha}$, $\vec{\beta}$ and $\vec{\gamma}$ are the static polarizability, the first order hyperpolarizability and the second order hyperpolarizability. The polarizability $\vec{\alpha}$ is the second-rank

†We want to avoid the higher multipoles and want to consider only first order perturbation.

cartesian tensor that characterizes the lowest-order induced dipole moment. The hyperpolarizabilities $\overset{\text{---}}{\beta}$ and $\overset{\text{---}}{\gamma}$ represent third and fourth-rank cartesian tensors. $\overset{\text{---}}{\alpha}$ and $\overset{\text{---}}{\beta}$ can be written as

$$\overset{\text{---}}{\alpha} = -\left(\frac{d^2 E}{d\vec{\mathcal{E}}^2}\right) \text{ and } \overset{\text{---}}{\beta} = -\left(\frac{d^3 E}{d\vec{\mathcal{E}}^3}\right). \quad (2.6)$$

From equation (2.6), it can be seen that the polarizabilities and the hyperpolarizabilities can be obtained by differentiating the energy E of the system with respect to the electric field $\vec{\mathcal{E}}$. The total energy of a system is defined by

$$E = \frac{\langle \psi | H_{elec} | \psi \rangle}{\langle \psi | \psi \rangle}. \quad (2.7)$$

where ψ is the wave function of the particle. The energy and wave function dependence on $\vec{\mathcal{E}}$ is determined using time-independent perturbation theory. This requires that for a given system and within a quantum mechanical formalism, we must compute the energy and wave function of the ground and first few excited states. We use HF, CIS and DFT formalisms to obtain these energies and wave functions. In the next few sections, we briefly discuss these methods.

2.2 The electronic Hamiltonian of a system

Consider a system of N electrons and K nuclei with charge Z_n . The Hamiltonian H of the system can be written as [48]

$$\begin{aligned}
 H = & \sum_{i=1}^N \frac{p_i^2}{2m} + \sum_{n=1}^K \frac{P_n^2}{2M_n} + \frac{1}{4\pi\epsilon_0} \frac{1}{2} \sum_{i,j=1; i \neq j}^N \frac{e^2}{|\vec{r}_i - \vec{r}_j|} \\
 & - \frac{1}{4\pi\epsilon_0} \sum_{n=1}^K \sum_{i=1}^N \frac{Z_n e^2}{|\vec{r}_i - \vec{R}_n|} + \frac{1}{4\pi\epsilon_0} \frac{1}{2} \sum_{n,n'=1; n \neq n'}^K \frac{Z_n Z_{n'} e^2}{|\vec{R}_n - \vec{R}_{n'}|}
 \end{aligned} \quad (2.8)$$

where i refers to the electrons and n to the nuclei, m is the mass of electron, and M_n are the masses of the different nuclei. The first term is the kinetic energy of the electrons, the second is the kinetic energy of the nuclei, the third is the Coulomb repulsion between the electrons and the fourth is the Coulomb attraction between electrons and nuclei and the last term is the Coulomb repulsion between the nuclei.

Equation (2.8) is complicated and if the numbers of electrons and nuclei are not small, it is impossible to solve the stationary Schrödinger equation for this Hamiltonian directly on even the largest and fastest computers available today. Since nuclei are much heavier than the electrons, we can assume that the nuclei move much more slower than the electrons. This

approximation is known as Born-Oppenheimer approximation [48]. Using Born-Oppenheimer approximation, the electronic and nuclear motions have been treated separately. The electronic Hamiltonian is given by

$$H = \sum_{j=1}^N \frac{p_j^2}{2m} + \frac{1}{2} \frac{1}{4\pi\epsilon_0} \sum_{i,j=1; i \neq j}^N \frac{e^2}{|\vec{r}_i - \vec{r}_j|} - \frac{1}{4\pi\epsilon_0} \sum_{n=1}^K \sum_{j=1}^N \frac{Z_n e^2}{|\vec{r}_j - R_n|}. \quad (2.9)$$

2.3 Hartree-Fock theory

The HF method is a variational method in which the wave functions of the many-electron system have the form of an anti-symmetrised product of one-electron wave functions to satisfy the Pauli-exclusion principle. This restriction leads to an effective Schrödinger equation for individual one-electron wave functions or orbitals with a potential determined by the orbitals occupied by the other electrons. That is, the HF method introduces an effective potential which depends on all the other electrons through their average Coulomb and exchange fields [49]. This coupling between the orbitals via the potentials causes the resulting equations to become nonlinear in the orbitals. The HF procedure is close in spirit to the mean-field approach used in statistical mechanics [48]. In this method, the correlations between the electrons are neglected to some extent and the Coulomb repulsion between the electrons is represented in an average way.

2.3.1 HF equations

The total wave function ψ which is an antisymmetrized product (Slater determinant) of single-electron wave functions (orbitals), is defined as [49]

$$\begin{aligned} \psi(1, 2, \dots, N) &= \frac{1}{\sqrt{N!}} \begin{vmatrix} \psi_1(1) & \psi_2(1) & \dots & \psi_N(1) \\ \psi_1(2) & \psi_2(2) & \dots & \psi_N(2) \\ \vdots & \vdots & & \vdots \\ \psi_1(N) & \psi_2(N) & \dots & \psi_N(N) \end{vmatrix} \\ &= \frac{1}{\sqrt{N!}} \det \{ \psi_1(1) \psi_2(2) \dots \psi_N(N) \} \end{aligned} \quad (2.10)$$

where the single-electron orbitals are given by

$$\psi_i(j) = \phi_i(\vec{r}_j) \chi_i(m_j). \quad (2.11)$$

$\phi_i(\vec{r}_j)$ and $\chi_i(m_j)$ are the spatial and the spin orbitals respectively. The spin orbitals are either α or β spin functions depending on whether $m_j = \pm 1/2$.

The HF energy with respect to the orbitals ϕ_i , is given by [49, 50]

$$\begin{aligned} E = \langle H \rangle &= \sum_i \int d^3 r \phi_i^*(\vec{r}) \left[-\frac{\hbar^2}{2m} \nabla^2 + V(\vec{r}) \right] \phi_i(\vec{r}) \\ &+ \frac{1}{2} \sum_{i,j} \int d^3 r d^3 r' \frac{e^2}{|\vec{r} - \vec{r}'|} |\phi_i(\vec{r})|^2 |\phi_j(\vec{r}')|^2 \\ &- \frac{1}{2} \sum_{i,j} \int d^3 r d^3 r' \frac{e^2}{|\vec{r} - \vec{r}'|} \phi_i^*(\vec{r}) \phi_i(\vec{r}') \phi_j^*(\vec{r}') \phi_j(\vec{r}) \delta_{m_i m_j}. \end{aligned} \quad (2.12)$$

Here $V(\vec{r})$ is the electrostatic potential due to the nuclei. Differentiating equation (2.12) with respect to the spin orbitals, we obtain nonlinear integro-differential HF equations

$$\hat{f}(\vec{r}) \phi_l(\vec{r}) = \lambda_l \phi_l(\vec{r}), \quad l = 1, 2, 3, \dots, N \quad (2.13)$$

where $\hat{f}(\vec{r})$ is the Fock operator and is given by

$$\hat{f}(\vec{r}) = -\frac{\hbar^2}{2m} \nabla^2 + V(\vec{r}) + v^{HF}(\vec{r}). \quad (2.14)$$

v^{HF} is the effective self-consistent single-particle potential which is produced by the direct and exchange Coulomb terms in equation (2.12). The eigenvalues λ_l are the Lagrange multipliers as introduced by the variational theorem and may correspond to the single-electron eigenvalues. These eigenvalues are used to approximate the removal energies of the i^{th} electron ("Koopmans theorem"[51]).

The entire set of single-particle wave functions must be solved simultaneously until self-consistency is achieved. This approach is called the self-consistent field (SCF) technique. The most commonly used form of HF theory involves the closed-shell single-determinant wave functions [52]. These wave functions are suitable for the description of the ground states of the molecules with an even number of electrons (n). The wave function is of singlet type, that is, it is an eigenfunction of the spin-squared operator, \hat{S}^2 , with zero eigenvalue. Since the same spatial orbitals are used for spin-up and spin-down electron, the HF method is referred to as restricted HF or RHF and this wave function is classified as spin restricted.

2.3.2 Basis set expansions of HF wave functions

A method that involves converting integro-differential HF equations to algebraic forms was introduced independently by Hall [53] and Roothaan [54]. Each molecular orbital (MO) $\phi_i(\vec{r}_k)$ is expressed as a linear combination of atomic orbitals (LCAO) [49], i.e.,

$$\phi_i(\vec{r}_k) = \sum_l^M c_{il} \varphi_l \quad (2.15)$$

where the atomic orbitals φ_l are chosen from some suitable set and in turn ϕ_i are often expressed in terms of basis set functions.

The molecular orbital depends on the size and choice of the basis set. In terms of atomic orbitals, the Coulomb direct and exchange integrals are of the following form

$$V_{ijkl} = \int d^3\vec{r} d^3\vec{r}' \phi_i^*(\vec{r}) \phi_j(\vec{r}') \frac{e^2}{|\vec{r} - \vec{r}'|} \phi_k^*(\vec{r}') \phi_l(\vec{r}). \quad (2.16)$$

The computational time in HF calculations go as M^4 (where M is the number of basis set wave functions), as equation (2.16) contains four molecular orbitals. Hence the computation time can be significantly decreased by limiting the size of the basis set.

For atoms and small molecules the basis set often used consists of Slater-type orbitals (STO) of the form

$$\varphi_{nlm}(r, \theta, \phi) = N r^{n-1} e^{-\gamma r} Y_{lm}(\theta, \phi) \quad (2.17)$$

where N and γ are constants and $Y_{lm}(\theta, \phi)$ is the m^{th} component of the l^{th} spherical harmonic. STO's have not been widely used for diatomic and polyatomic molecules because it is very difficult and time-consuming to evaluate multi-center electrostatic integrals of the form given in equation (2.16). Instead, Gaussian-type orbitals (GTO) are used for polyatomic molecules as was first suggested by Boys [55]. Cartesian GTO's are of the form

$$\varphi_{tuv}(\vec{r}) = N x^t y^u z^v e^{-\gamma r^2} \quad t, u, v = 0, 1, 2, 3, \dots \quad (2.18)$$

where N and γ are constants as above.

The main advantage of GTO's in calculating the polarizabilities is that all integrals like equation (2.16) can be evaluated analytically but the disadvantage is that large basis sets are needed since atomic orbitals are not well approximated by just a few Gaussian functions.

2.4 Configuration interaction singles

The multiple-determinant wave function for the configuration interaction is constructed by starting with the HF wave function and making new

determinants by moving the electrons from the occupied to unoccupied orbitals [56]. With all the possible excitations, the configuration interaction calculation is called a full CI. If only one electron is moved for each determinant, then it is called the configuration interaction single-excitation calculation (CIS). This is the most common way to obtain excited state energies. This configuration interaction calculation uses the molecular orbitals that have been optimized in the HF calculation. A CIS calculation begins with the initial set of HF orbitals and promotes a single electron to one of the virtual (unoccupied) orbitals. This procedure gives the description of the excited states of the molecule without changing the quality of the description of the ground state. A brief discussion of CIS wavefunction follows in section 2.4.1.

2.4.1 CIS wave functions

Suppose the single-determinant HF wave function ψ_0 is defined as [57]

$$\psi_0 = (n!)^{-1/2} | \chi_1 \chi_2 \chi_3 \chi_4 \dots \chi_n | \quad (2.19)$$

where $\chi_1, \chi_2, \chi_3, \dots, \chi_n$ are the occupied spin orbitals. Let ψ_s be the determinantal wave functions with $s > 0$. ψ_s may be constructed by replacing one or more of the occupied spin orbitals χ_i, χ_j, \dots in

equation (2.19) by the virtual spin orbitals χ_a, χ_b, \dots . The wave functions ψ_s can be classified into single-substitution functions, ψ_i^a , in which χ_i is replaced by χ_a , double-substitution functions, ψ_{ij}^{ab} in which χ_i is replaced by χ_a and χ_j is replaced by χ_b , and so forth. This series of substituted determinants goes all the way to n-substituted terms in which all the occupied spin orbitals are replaced by the virtual spin orbitals.

In the full configuration interaction method, a trial wave function can be written as [57]

$$\psi = a_0 \psi_0 + \sum_{s>0} a_s \psi_s \quad (2.20)$$

where the summation $\sum_{s>0}$ is over all substituted determinants. The unknown coefficients, a_s , can be obtained by the linear variational method, and are given by

$$\sum_s (H_{st} - E_t \delta_{st}) a_{st} = 0 \quad t = 0, 1, 2, \dots \quad (2.21)$$

Here, H_{st} is the configuration matrix element and is defined by

$$H_{st} = \int \dots \int \psi_s H \psi_t d\tau_1 d\tau_2 \dots d\tau_n \quad (2.22)$$

and E_t is the energy. The lowest root E of equation (2.22) gives to the energy of the electronic ground state. If no substitutions are permitted, $\psi = \psi_0$, corresponding to the HF solution.

The CIS wave function is obtained with single substitution functions only and is given by

$$\Psi_{CIS} = a_0 \Psi_0 + \sum_i^{\text{occ}} \sum_a^{\text{virt}} a_i^a \Psi_i^a. \quad (2.23)$$

In the CIS framework, the calculation of static dipole polarizabilities is done by the finite field method [49]. The perturbation of a small but finite external field, equation (2.1), is added to the Hamiltonian. The change in energy or the induced dipole moment is calculated for a series of electric field strengths. Then the polarizability is computed from numerical differentiation by equation (2.6).

2.5 Density functional theory

DFT is built upon two fundamental theorems as proposed by Hohenberg and Kohn [58]. The first theorem states that all the ground state properties of an electron are fully determined by the electronic density distribution $n(\vec{r})$ which is given by [49]

$$n(\vec{r}) = |\Psi_0|^2 \quad (2.24)$$

where Ψ_0 is the ground state wave function. Then the ground state energy E is a unique functional of the density and is defined by

$$E[n] = T[n] + \int [v_i(\vec{r}) + v_{ext}(\vec{r})]n(\vec{r})d^3r + \frac{1}{2} \int \frac{n(\vec{r})n(\vec{r}')}{|\vec{r} - \vec{r}'|} d^3r d^3r' + E_{xc}[n] \quad (2.25)$$

where the first term is the kinetic energy function, the second and the third is the energy due to the ionic $v_i(\vec{r})$ and externally applied $v_{ext}(\vec{r})$ fields, the fourth is the direct electron-electron Coulomb interaction term and the last term is the exchange-correlation functional.

The exchange- correlation functional E_{xc} can be written as

$$E_{xc} = E_x + E_c \quad (2.26)$$

where E_x is the exchange interaction and E_c is the correlation energy functional.

The Hohenberg-Kohn first theorem states that the functionals must exist but they give no information about their specific forms. Many approximations have been proposed for E_x and E_c functionals. The second Hohenberg-Kohn theorem states that variational principle can be applied to the energy functional in order to obtain ground state electron density and energy [58]. One scheme for applying the variational principle involves expanding the density $n(\vec{r})$ in terms of a set of single particle wave functions. This formalism is known as Kohn-Sham (KS) theory. In the next section we briefly outline this approach.

2.5.1 KS formalism

Kohn and Sham states that the electron density can be written as a complete set of single particle “wave functions” as follows [49]

$$n(\vec{r}) = \sum_{i=1}^N |\phi_i(\vec{r})|^2 \quad (2.27)$$

where the summation goes over the N lowest states. If the energy functional equation (2.25) is minimized with respect to the electron density (equation 2.27), a set of Schrödinger-like equations are produced

$$\left[-\frac{\hbar^2}{2m} \nabla^2 + v_{\text{eff}}(\vec{r}) \right] \phi_i(\vec{r}) = \lambda_i \phi_i(\vec{r}) \quad (2.28)$$

where

$$v_{\text{eff}}(\vec{r}) = v_l(\vec{r}) + v_{\text{ext}}(\vec{r}) + \frac{\delta E_{xc}[n]}{\delta n(\vec{r})} \quad (2.29)$$

where the last term is the functional derivative of the exchange-correlation functional. Equations (2.28) are called the KS equations.

There is a strong similarity between the KS equations and those that arise in HF theory. In the DFT, the calculation of static dipole polarizabilities is done by the finite field method [49]. Hence the polarizability is computed from numerical differentiation of equation (2.6).

Within the time independent perturbation theory the following two approaches can be used to calculate the polarizability and hyperpolarizability of the system

- (a) Compute the energy derivatives (equation (2.6)) explicitly (analytically or numerically).
- (b) Use SOS or sum over oscillator strengths formalism.

In the next two sections we briefly discuss these two approaches.

2.6 Energy derivatives formulation

Analytic or numerical differentiation of the molecular energy is needed to calculate the polarizability and hyperpolarizability as noted in equation (2.6). As an example, we focus on polarizabilities calculated using CIS wave functions. Gaussian (03, 98 and 94) [42, 43, 59] were used to calculate the analytic polarizabilities which are exact within the CIS framework. We outline the calculation of the derivatives and hence the theoretical framework employed in the Gaussian (03, 98 and 94) [42, 43, 59] to calculate CIS polarizabilities [60].

For the CIS method, the CIS energy is given by

$$E_{CIS} = \frac{\langle \Psi_{CIS} | H_{elec} | \Psi_{CIS} \rangle}{\langle \Psi_{CIS} | \Psi_{CIS} \rangle}. \quad (2.30)$$

The CIS energy is obtained variationally by optimizing the CIS expansion coefficients [61]. This energy is then differentiated with respect to the electric field.

The normalized wave function is

$$\psi_{CIS} = \sum_S a_S \psi_S = a_0 \psi_0 + \sum_i^{\text{occ}} \sum_a^{\text{virt}} a_i^a \psi_i^a \quad (2.31)$$

where ψ_0 is the HF determinant. The second term in equation (2.31) comes from the sum over the single excitations where ψ_i^a are singly substituted Slater type determinants. All the determinants are antisymmetrized products of MO's which are eigenfunctions of the Fock operator. The Fock operator is given as a linear combination of a set of basis functions, ϕ_λ with expansion coefficients c_λ . CIS coefficients are adjusted variationally to minimize the CIS energy (equation 2.30) [61].

The CIS wave function is completely specified by a set of parameters which include the CIS coefficients and the molecular orbital expansion coefficients. Both sets of coefficients are in general dependent on the external perturbation electric field. The CIS wave function is also dependent upon the other parameters such as geometry and basis set choice, however, these are taken to be independent of the external perturbation. Using the perturbed Hamiltonian (equation 2.1), it is obtained[60]

$$\left(\frac{dE_{CIS}}{d\bar{E}}\right)_0 = \langle \psi_{CIS} | \bar{\mu} | \psi_{CIS} \rangle + \sum_s \frac{\partial E_{CIS}}{\partial a_s} \frac{\partial a_s}{\partial \bar{E}} + \sum_{\lambda_p} \frac{\partial E_{CIS}}{\partial c_{\lambda_p}} \frac{\partial c_{\lambda_p}}{\partial \bar{E}} \quad (2.32)$$

Here, CIS coefficients a_s are chosen to minimize the CIS energy,

therefore, $\left(\frac{\partial E_{CIS}}{\partial a_s}\right) = 0$. But the molecular orbital coefficients c_{λ_p} are

chosen to minimize the HF energy not the CIS energy, therefore,

$\left(\frac{\partial E_{CIS}}{\partial c_{\lambda_p}}\right) \neq 0$. Thus the second term on the right hand side of equation

(2.32) is zero. Hence, equation (2.32) can be written as

$$\left(\frac{dE_{CIS}}{d\bar{E}}\right)_0 = \langle \psi_{CIS} | \bar{\mu} | \psi_{CIS} \rangle + \sum_{\lambda_p} \frac{\partial E_{CIS}}{\partial c_{\lambda_p}} \frac{\partial c_{\lambda_p}}{\partial \bar{E}} \quad (2.33)$$

Equation (2.33) shows the breakdown of FH theorem for CIS systems.

2.7 Sum over states

To compute the polarizability of the system by using equation (2.6), we need to know the perturbation expression for the energy. The perturbed energy is given by [46]

$$E_0 = E_0^{(0)} + \langle \psi_0 | H' | \psi_0 \rangle + \langle \psi_0 | H'' | \psi_0 \rangle + \sum_n' \frac{\langle \psi_0 | H' | \psi_n \rangle \langle \psi_n | H' | \psi_0 \rangle}{E_0 - E_n} + \dots \quad (2.34)$$

where ψ_0 is the ground state wave function of energy E_0 and ψ_n is the excited state wave function of energy E_n and H'' is the second-order Hamiltonian perturbation. In our case, there is no second-order Hamiltonian perturbation, so the third term has no contribution (see equation 2.1).

Substituting H' from equation (2.1), into equation 2.34, we get

$$E_0 = E_0^{(0)} - \langle \psi_0 | \bar{\mu} | \psi_0 \rangle \cdot \bar{\epsilon} + \sum_n' \left\{ \frac{\langle \psi_0 | \bar{\mu} | \psi_n \rangle \langle \psi_n | \bar{\mu} | \psi_0 \rangle}{E_0 - E_n} \right\} \cdot \bar{\epsilon}^2 + \dots \quad (2.35)$$

By taking the first and the second derivative of equation (2.35) with respect to the electric field $\bar{\epsilon}$ and setting $\bar{\epsilon} = 0$, we have found respectively

$$\left(\frac{d E_0}{d \bar{\epsilon}} \right)_0 = - \langle \psi_0 | \bar{\mu} | \psi_0 \rangle = \bar{\mu}_0 \quad (2.36)$$

and

$$\left(\frac{d^2 E_0}{d \bar{\epsilon}^2} \right)_0 = -2 \sum_n' \frac{\langle \psi_0 | \bar{\mu} | \psi_n \rangle \langle \psi_n | \bar{\mu} | \psi_0 \rangle}{E_0 - E_n} \quad (2.37)$$

Equation (2.36) states that the permanent electric dipole of the molecule is the expectation value of the dipole moment operator in the unperturbed state of the system. Equation (2.37) is the polarizability of the molecule in terms of integrals over its wave function.

Hence the polarizability of the system can be written as

$$\tilde{\alpha} = -2 \sum_n' \frac{\langle \psi_0 | \tilde{\mu} | \psi_n \rangle \langle \psi_n | \tilde{\mu} | \psi_0 \rangle}{E_0 - E_n}. \quad (2.38)$$

The prime indicates that the summation excludes the ground state. If we use the perturbation theory to second order, we can get the expression for the first order hyperpolarizability $\tilde{\beta}$. As given by [34]

$$\tilde{\beta} = 6 \sum_n \sum_l \frac{\langle \psi_0 | \tilde{\mu} | \psi_n \rangle \langle \psi_n | \tilde{\mu} | \psi_l \rangle^- \langle \psi_l | \tilde{\mu} | \psi_0 \rangle}{(E_0 - E_n)(E_0 - E_l)} \quad (2.39)$$

where $\langle \psi_n | \tilde{\mu} | \psi_l \rangle^- = \langle \psi_n | \tilde{\mu} | \psi_l \rangle - \langle \psi_0 | \tilde{\mu} | \psi_0 \rangle \delta_{nl}$.

At this point, we will focus our discussion on the expression for the polarizability (equation 2.38). Often, we are interested in the mean polarizability of our molecule (since in many experimental situations molecules are randomly oriented in bulk states). We have assumed that the diagonal elements of the polarizability matrix; α_{xx} , α_{yy} and α_{zz} have the largest contribution to the polarizability tensor.

By setting the matrix element $\langle \psi_0 | \bar{\mu} | \psi_n \rangle \equiv \bar{\mu}_{0n}$ and $\Delta E_{n0} = E_n - E_0$; and with equation (2.38), the components α_{xx} , α_{yy} and α_{zz} can be written as

$$\begin{aligned}\alpha_{xx} &= 2 \sum_n' \frac{\mu_{x,0n} \mu_{x,n0}}{\Delta E_{n0}} \\ \alpha_{yy} &= 2 \sum_n' \frac{\mu_{y,0n} \mu_{y,n0}}{\Delta E_{n0}} \\ \alpha_{zz} &= 2 \sum_n' \frac{\mu_{z,0n} \mu_{z,n0}}{\Delta E_{n0}}\end{aligned}\quad (2.40)$$

Hence, the average polarizability of the system can be written as

$$\begin{aligned}\bar{\alpha}_{avg} &= \frac{1}{3} (\alpha_{xx} + \alpha_{yy} + \alpha_{zz}) \\ &= \frac{2}{3} \sum_n' \frac{\mu_{x,0n} \mu_{x,n0} + \mu_{y,0n} \mu_{y,n0} + \mu_{z,0n} \mu_{z,n0}}{\Delta E_{n0}} \\ &= \frac{2}{3} \sum_n' \frac{\bar{\mu}_{0n} \cdot \bar{\mu}_{n0}}{\Delta E_{n0}}.\end{aligned}\quad (2.41)$$

Since $\bar{\mu}$ is a hermitian operator, we can write $\bar{\mu}_{0n} = \bar{\mu}_{n0}^*$. Hence, equation (2.41) can be written as

$$\bar{\alpha}_{avg} = \frac{2}{3} \sum_n' \frac{|\mu_{n0}|^2}{\Delta E_{n0}}.\quad (2.42)$$

It can be noticed from equation (2.42) that the polarizability depends on the square of the transition dipole moments.

A quantity called the oscillator strength, f_{n0} , can be defined as follows

$$f_{n0} = \left(\frac{4 \pi m_e}{3 e^2 \hbar} \right) \nu_{n0} |\mu_{n0}|^2$$

where ν_{n0} is the transition frequency. Thus using equation (2.41) the average polarizability of the system can be given by

$$\bar{\alpha}_{avg} = \frac{\hbar^2 e^2}{m_e} \sum_n \frac{f_{n0}}{\Delta E_{n0}^2}. \quad (2.43)$$

Once the oscillator strengths are computed for a given molecule, we can estimate the average polarizability. Within the SOS formalism of the electronic polarizability, the largest contributions correspond to the largest oscillator strengths which in turn correspond to the 'strongest' transitions in a molecule.

From the above discussion, we could see that the energy derivative formalism is a better approximation to the polarizability than the SOS since an exact expression for the polarizability includes two terms (see equation (2.33)). The second term is missing in the SOS formalism. On the other hand SOS approximation satisfies FH theorem. Whereas, due to the presence of the second term (see equation (2.33)), there is a breakdown of the FH theorem for CIS method.

Chapter 3

COMPUTATIONAL APPROACH

3.1 Computational details

In the first part of this thesis (see Chapter 4), the oligomers ranging from monomer to the octamer (or in some cases longer oligomers up to 16 rings) of OTH, OCY, OFV, OCNTH, OPCNCY and OPCNFV were fully geometry optimized to investigate the chain length dependence of α and excitation energies. The investigations have been carried out for the SOS and CIS methods. In the second part of the thesis (see Chapter 5), partial geometry optimizations of oligomers OA, OTH, OCY, OFV and OCNTH have been performed by using RHF, CIS and DFT methods to see the effect of BLA on α , β and excitation energies. For OA we have considered two oligomers with 7-bonds and 9-bonds and for OTH, OCY, OFV and OCNTH we considered unit cells consisting of two rings or dimers. We use -H as end groups for the aromatic isomers and =H₂ and =CH₂ as end groups for the quinonoid isomers. We have used =CH₂ end groups in quinonoid isomers in order to have the same number of double

bonds in both aromatic and quinonoid isomers. The =CH₂ end groups in quinonoid isomers distort the symmetry of the dimers. The dimers are no longer centro-symmetric.

The optimization is performed in the internal coordinates (Z-matrix). In the full optimizations, all specified variables are optimized in order to find the lowest energy structure, while in the partial optimizations, only a specified subset of variables are optimized. The subset of variables whose values should be constant is specified in a separate input section [42, 43, 59]. In this process, we have kept the bond lengths along the chain backbone fixed and allowed all other variables to be optimized.

In the computations, we have used three versions of Gaussian software (94, 98 and 03) [42, 43, 59]. Gaussian is a large *ab initio* program that can execute batch jobs. It incorporates the widest range of functionality of any *ab initio* code [62] and uses one of the simplest ASCII input file formats. We have used the graphic interface Gauss View [63] for building molecules, creating Gaussian input files and viewing the results.

The basis set is very important and should be considered very carefully for *ab initio* calculations of the polarizabilities and hyperpolarizabilities [64]. We have chosen the split-valence 3-21G* basis set for our investigations. That is, α and β calculations have been performed using the split-valence 3-21G* basis set. This basis set was chosen because smaller basis sets require less computing time and allowed us to perform computation on larger molecules. Thus, in order to be consistent, we have used the same (smaller)

basis set for both the larger and smaller compounds. Previous studies showed that this basis set is adequate for computing excitation energies of extended π -conjugated oligomers [22, 39]. In addition, most of the contributions to the polarizabilities come from the longitudinal component [26, 27] and it was found by Archibong and Thakkar that small basis sets are very suitable for the longitudinal properties [23].

We have determined the BLA values by calculating δr . δr is defined as the average of the difference between the neighboring single and double carbon-carbon bonds. δr is positive for the quinonoid structures and negative for the aromatic structures. The value of δr is closely related to the band gap [22]. For OA, OTH, OCY and OFV unit cells (see figure 1.1), δr is defined as [22]

$$\delta r = \frac{1}{2} [(C_{\alpha'-\beta'}) - (C_{\beta'-\beta}) + (C_{\beta-\alpha}) - (C_{\alpha-\alpha'})] \quad (3.1)$$

and for the cyano-substituted derivative OCNTH unit cell (see figure 1.1), δr is given by

$$\delta r = \frac{1}{4} \left[\begin{array}{l} (C_{\alpha'-\beta'}) - (C_{\beta'-\beta}) + (C_{\beta-\alpha}) - (\text{Intracell}) + (C_{\alpha_1-\beta_1}) \\ - (C_{\beta_1-\beta'_1}) + (C_{\beta'_1-\alpha'_1}) - (\text{Intercell}) \end{array} \right] \quad (3.2)$$

The difference in π -bond orders between adjacent bonds defines BOA, which is directly related to BLA in conjugated π -electron compounds. Meyers *et al.* found a very small difference between BLA and BOA [32].

We have used the same keywords in Gaussian Software for all oligomers when computing polarizabilities and hyperpolarizabilities. The keywords (see table 7.2 in the Appendix) for CIS method are TRCIS, Opt, Freq and Polar (full and partial optimization); for HF method are Opt = Z-matrix, Freq and Polar (partial optimization); and for DFT method are RB3PW91, Opt = Z-matrix, Freq = Raman and Polar (partial optimization). It is important to note that we have computed the static electronic contribution to the polarizability. We have calculated the average polarizability α by taking the average of the three components, α_{xx} , α_{yy} and α_{zz} as we have seen that those components are the most dominant components in the polarizability calculations. Hence the average polarizability is given as follows (also see equation 2.41)

$$\bar{\alpha}_{avg} = \frac{1}{3} (\alpha_{xx} + \alpha_{yy} + \alpha_{zz}) \quad (3.3)$$

in both SOS and CIS methods. Two SOS calculations have been performed using CIS values for excitation energies and oscillator strengths. No tensor components have been calculated when approximate average α has been tabulated. In this case, equation (2.43) is used directly to estimate the average α . In the second case, the tensor components have been determined and both equations (2.43) and (3.3) have been used to estimate the average α . It should be mentioned that in our computations, β has been computed automatically for HF and DFT methods using the keyword Polar [42, 43 and 59] but for CIS, although we have used the keyword (see table 7.2 in Appendix) Polar = EnOnly, to produce β which is suggested by the Gaussian 03 User's Reference [59], we have not obtained the results.

Hence, for β only HF and DFT results have been obtained. Data obtained for α and β (see Appendix) have been determined in the standard orientation (the origin of this coordinate system corresponds to the center of mass of the molecule) and the input (Z-matrix) orientation coordinate system respectively. For HF, we have obtained the data for β in both orientations [65] but not for DFT. To maintain consistency between the two methods, data for β have been tabulated (see in the Appendix) only for the Z-matrix orientation. α and β have been measured in atomic units. For the electric polarizability, 1a.u. = $1.648777 \times 10^{-41} \text{ C}^2 \text{m}^2 \text{J}^{-1}$ and for the first order hyperpolarizability, 1a.u. = $3.206 \times 10^{-51} \text{ C}^3 \text{m}^3 \text{J}^{-2}$ [66].

We have used two ways to compute the excitation energies of the polymers. We have estimated the excitation energies from the difference between ionization potentials (IP) and electron affinities (EA). IPs and EAs have been obtained respectively from the negative of the HOMO and the LUMO energies in the HF and DFT calculations. In CIS calculations, excitation energies have been calculated from the total energy difference between the ground state and first excited state.

For the DFT calculations, the hybrid functionals mix some SCF (HF) exchange with the DFT exchange. There have been many hybrid functionals proposed for *ab initio* calculations such as B3LYP, B3P86 etc. We have chosen the B3PW91 functional as it was found in other investigations that all the hybrids give approximately similar results and B3PW91 results agree well with the experimental values when this comparison can be made [67].

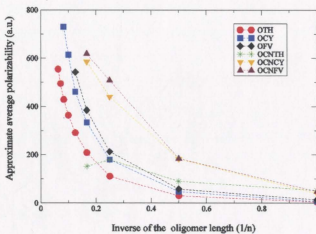
Chapter 4

POLARIZABILITY VS CHAIN LENGTH

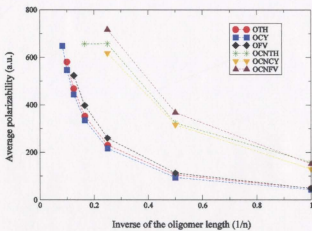
In this chapter, we discuss trends in polarizabilities of the studied systems for both SOS and CIS methods as discussed in Chapters 2 and 3. First, in section 4.1, we describe the dependence of the polarizabilities on the inverse of the oligomer length, then in section 4.2 the dependence of the polarizabilities per monomer on the oligomer length and lastly in section 4.3, we describe the evolution of the excitation energy as function of the polarizabilities.

4.1 Polarizability vs the monomer length - infinite chain length limit

The calculated polarizabilities for OTH, OCY, OFV, OCNTH, OCNCY and OCNFV in SOS and CIS methods are tabulated in tables 6.1 and 6.2 (see Appendix). The main objective of this study is to investigate the variation of polarizabilities as function of oligomer lengths. We have found



(a)



(b)

Figure 4.1: (a) Approximate average and (b) average polarizability as a function of the inverse of the oligomer length in SOS method.

that it is more informative to plot polarizabilities as function of the inverse of the oligomer length rather than as function of the oligomer length. This procedure allows us to see clearly what happens when the chain length, n , becomes very large because in this limit $1/n$ goes to zero. Figures 4.1 and 4.2a show the polarizabilities as function of the inverse of the oligomer lengths in SOS and CIS methods. From the tables and figures, it can be noted that the magnitudes of the CIS polarizabilities are greater than those of the SOS polarizabilities. In all cases, for a specific oligomer, the magnitude of polarizability increases with the increase of the oligomer length.

Figure 4.1 shows that in the SOS method both the average α and the approximate average α give very similar trends of α as function of $1/n$. The average polarizability is calculated from the average of the diagonal elements of the polarizability tensor and the approximate average polarizability is calculated from oscillator strengths. In both cases the cyano substituted oligomers are clustered above their parent oligomers with one exception for the approximate average α , OCNTH is placed amongst the parent oligomers. However, in both cases OCNTH displays leveling off of α on going from tetramer to seximer. The results for the CIS polarizabilities (see figure 4.2a), except for the fact that their magnitudes are 2 to 4 times larger than the SOS values, exhibit very similar trends. The three cyano compounds are clustered above their parent oligomer curves and OCNTH again displays a decrease in α on going from 4 to 6-monomer chains.

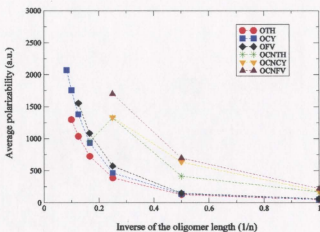


Figure 4.2 a: Average polarizability as a function of the inverse of the oligomer length in CIS method.

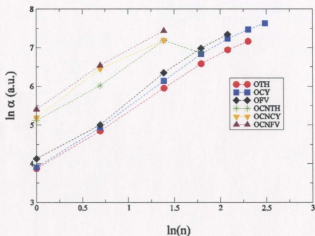


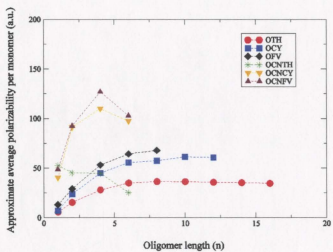
Figure 4.2 b: $\ln(\text{average polarizability})$ as a function of the $\ln(\text{oligomer length})$ in CIS method.

The shape of most of the curves is approximately same (see figure 4.2a). The one exception being is OCNTH, where the compound initially exhibits same dependence of α on $1/n$ and then α drops off. As two methods have shown the same trends (figures 4.1 and 4.2a), to see the dependence of the average polarizability on the oligomer length, we have only plotted figure 4.2b for CIS method. It has observed that the average polarizability varies as $n^{1.4}$ to $n^{1.5}$ for all except for OCNTH for which α varies $n^{1.1}$. Further computations of α were prohibitive for larger compounds. However, our guess would be that after the initial drop, α would increase at a rate that is similar to the one observed for OTH. There is some support for this idea when one looks closely at the table 6.2. In particular it can be noted from table 6.2 that most of the contributions to the average polarizability in most cases come from the longitudinal component of the polarizability (which is along the x direction). In the case of OCNTH, there is a significant decrease in α_{xx} on going from 4 to 6 monomers. It is, as if, the cyano group contribution becomes less important when the chain becomes longer and only the thiophene rings contribute to the polarizability.

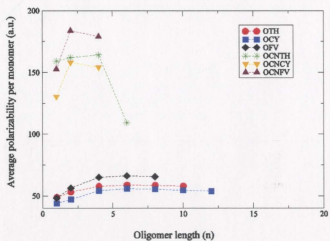
4.2 Polarizability per monomer vs oligomer length

Figures 4.3 and 4.4 show that initially the polarizability per monomer (α/n) increases with the increase of the oligomer length for all the systems and then after certain oligomer length it either levels off or decreases. It has been found that for both SOS and CIS methods, for OTH and OCY, the α/n increases with the increasing oligomer length up to octamer and after that it remains approximately constant (see figures 4.3 and 4.4 and tables 6.1 and 6.2 in Appendix). For OFV, we have found that α/n increases with the increase of the oligomer length but as we have stopped our calculations at an octamer, we could only speculate, based on similarities in the behavior of OTH and OCY, that α/n would become constant as oligomer becomes even longer.

We have investigated α/n for OCNTH for oligomers made of monomer to seximer and have found different behaviors for the two methods. For the SOS method, with the increase of the oligomer length, the approximate average α/n decreases up to seximer and the average α/n first increases up to tetramer then it decreases for seximer. For CIS, we can see that with the increase of the oligomer length, α/n increases up to tetramer and then decreases. We have investigated α/n for OCNCY and OCNFV from monomer to seximer and from monomer to tetramer for SOS and CIS methods respectively. In both methods, with the increase of the oligomer



(a)



(b)

Figure 4.3: (a) Approximate average and (b) average polarizability per monomer as a function of the oligomer length in SOS method.

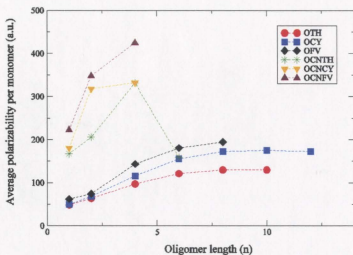


Figure 4.4: Average polarizability per monomer as function of the oligomer length in CIS method.

length, the α/n increases up to tetramer. For SOS, we have continued our investigation up to seximer, we have seen that with the increase of the oligomer length, there is a decrease in approximate average α/n . In all cases we can see that there is a large difference in magnitude of the calculated SOS and CIS polarizability per monomer.

4.3 Polarizability and excitation energy

First, we investigated the dependence of the excitation energies on the chain length of the polymers from monomer to higher length (see figure 4.5). For OTH, with the increase of the oligomer length, the excitation energies decrease up to octamer but after that seemed to be constant. OCY and OFV show similar behavior as OTH. For OCNCY and OCNFV, with the increase of the oligomer length, the excitation energies decreased. OCNTH has shown a different behavior than others. With the increase of the oligomer length, the excitation energy first decreases then slightly increases. Due to the calculation limitations, we could not continue our calculations for the longer oligomers for these molecules. Our investigations suggest that to clearly see the saturation effect, it is required to continue calculations for higher oligomer lengths.

We have found that there is an inverse relationship between the excitation energies and the polarizabilities of the polymers (see table 6.3 in Appendix). That is for all molecules with the increase of the oligomer length, the excitation energy decreases [37, 38] but the polarizability per monomer increases except where there is a variation at seximer for OCNTH (see table 6.3). In this case, with the increase of the oligomer length the excitation energy increases but the polarizability decreases. Our results for the excitation energies (see table 6.3) indicate that the effective

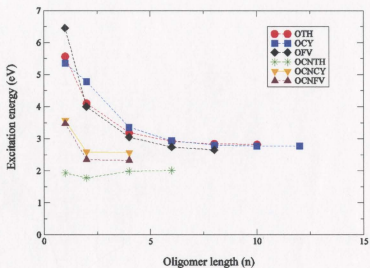


Figure 4.5: Excitation energy as a function of the oligomer length in CIS method.

length or mean conjugation length for OTH and OCNTH is approximately 8 to 10 monomers, and 4 to 6 monomers respectively, which corresponds to the saturation values of 2.837 eV and 1.987 eV, respectively. Chakraborty *et al.* have found the same results in their investigations [39]. The mean conjugation length for OCY and OFV, and OCNCY and OCNFV is around 8 monomers and 4 monomers respectively. They found the saturation values of 2.806 eV, 2.650 eV, 2.568 eV and 2.319 eV for these systems respectively. Our results are the same as those reported by Chakraborty *et al.* [22]. To see the relation between the excitation energy and the polarizability, we have plotted the excitation

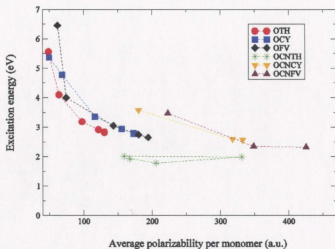


Figure 4.6: Excitation energy as a function of the polarizability per monomer in CIS method

energies as a function of the polarizability per monomer in figure 4.6. This figure shows that as the excitation energies decrease the polarizabilities per monomer increase with the increase of the oligomer length. Parent oligomers have higher excitation energies and lower polarizabilities than their cyano derivatives.

Chapter 5

POLARIZABILITY

VS

BOND LENGTH ALTERNATION

Partial geometry optimizations† on oligomers OA, OTH, OCY, OFV and OCNTH have been performed by using HF, CIS and DFT methods. We were interested to see the evolution of the α , β and ΔE with respect to BLA.

In order to see the effect of BLA upon α and β , we have systematically changed or modified the structures by simultaneously shortening all the single bond lengths and lengthening all the double bond lengths by steps of 0.02Å until they are equal and then reversed the process. This procedure produced two isomeric forms: aromatic ($\delta r < 0$) and quinonoid ($\delta r > 0$).

In this chapter we investigate the BLA effects upon α , β and ΔE for OA, OTH, OCY, OFV and OCNTH in sections 5.1, 5.2, 5.3 and 5.4 respectively.

†See Chapter 3.

5.1 OLIGOACETYLENE (OA)

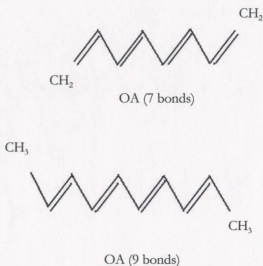


Figure 5.1: OA with 7 and 9 C-C bonds respectively.

We began the investigation of OA by generating acetylene oligomers of equal number of bonds but different end groups for the two oligomers. It was found that the end groups and number of double bonds have significant effects on the polarizabilities. To circumvent these problems, we studied OA consisting 7-bonds and 9-bonds. In each case, the oligomers have four double bonds and the same groups ($=\text{CH}_2$ for 7-bonds and $-\text{CH}_3$ for 9-bonds oligomers) at the end (see figure 5.1). It has also been observed that the single bonds do not have large effects on the

polarizabilities. We have considered two sets of OA with δr ranging between -0.17 \AA to 0 \AA and 0.03 \AA to 0.19 \AA . Our results are summarized in sections 5.1.1, 5.1.2 and 5.1.3.

5.1.1 Average polarizability per C-C bond vs bond length alternation

From figure 5.2, for the three computational methods, we observe that α per C-C bond (from now onward it will be referred as α/bond) increases as δr increases from -0.17 \AA to 0 \AA and then decreases as δr increases from 0.03 \AA to 0.19 \AA . The actual values plotted in figure 5.1 are given in table 1.1 in the Appendix. In all cases, α/bond has a maximum value at $\delta r = 0 \text{ \AA}$ (cyanine limit).

All methods show the same trend but they differ in the magnitude of α/bond . For RHF and DFT, α/bond has approximately the same magnitude. The magnitude of α/bond found by CIS is found to be greater by a factor ~ 1.5 (see table 1.1 in the Appendix). In the coordinate system, in which the calculations of α are carried out, x is the direction along the oligomer backbone, and y is perpendicular to the xz plane. The components α_{yy} , α_{zz} and α_{xy} are smaller than α_{xx} . α_{yz} and α_{zx} are nearly zero in magnitude (see table 1.1 in Appendix).

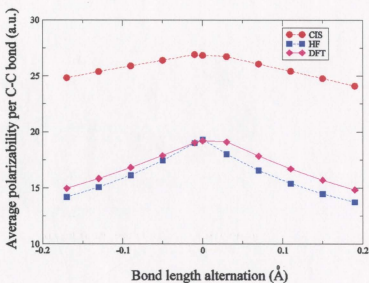


Figure 5.2: Evolution of average polarizability per C-C bond as a function of the bond length alternation for 7 ($BLA \leq 0$) and 9 ($BLA > 0$) C-C bonds of OA.

In all methods, α_{xx} is the largest. This clearly indicates that the largest contributions to α comes from its longitudinal component α_{xx} . This is due to the fact that because of π conjugation, electron redistribution in the presence of an electric field occurs most easily along the backbone of the oligomer. Similar trend, as seen in figure 5.2 (α/bond increases when δr tends to zero), has been found by Meyers *et al.* [32].

5.1.2 First order hyperpolarizability vs bond length alternation

From figure 5.3 and table 1.2 (see Appendix) we can see that for both the methods, with the increase of δr from -0.17 \AA to 0 \AA and 0.03 \AA to 0.19 \AA the first order hyperpolarizability increases, but there is a drop near $\delta r = 0 \text{ \AA}$. That is, β_{xxx} (and β_{zzz}) drops around $\delta r = 0 \text{ \AA}$ but not exactly at $\delta r = 0 \text{ \AA}$. It has been observed that the HF and DFT methods show the same trend but give different magnitudes for β . The β data (table 1.2 in the Appendix) for the two computational methods are given in the Z-matrix orientation coordinate systems. In this coordinate system x and z axes are in the plane of the oligomer and the oligomer is at an angle relative to x and z axes, and y axis is perpendicular to the xz plane. With the increase of δr , different components have shown different behaviors. β_{xxy} , β_{xyy} , β_{yyy} , β_{yyz} and β_{yzz} components are very small and change very little with δr . On the other hand, the magnitudes of β_{xxx} , β_{xyz} and β_{zzz} components are significantly larger as the molecule is in the xz plane and the contribution to β comes from both the x and z directions. β_{xxx} and β_{zzz} have the largest magnitudes of all the tensor components of $\overset{\equiv}{\beta}$ (hence they are plotted in figure 5.3). Of those two, β_{zzz} is the most dominant component (see in table 1.2 in Appendix).

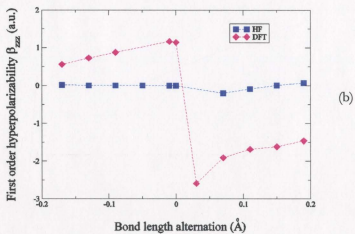
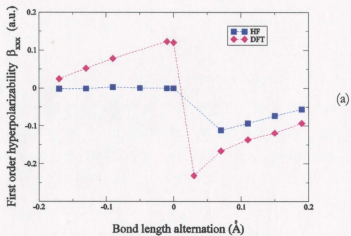


Figure 5.3: Evolution of first order hyperpolarizability (a) β_{xxx} and (b) β_{zzz} as a function of the bond length alternation for 7 ($\text{BLA} \leq 0$) and 9 ($\text{BLA} > 0$) C-C bonds of OA.

5.1.3 Excitation energy vs bond length alternation

From figure 5.4 and table 1.3 (see Appendix), we observe that the three computational methods give excitation energies (ΔE) that decrease as δr increases from -0.17 \AA to 0 \AA and then increase as δr increases from 0.03 \AA to 0.19 \AA . In other words, for both oligomers, ΔE decreases as δr tends to zero. CIS and DFT give comparable values for the excitation energies. HF values for excitation energy are larger by factors ~ 3 and ~ 2 than those obtained with DFT and CIS methods respectively (see table 1.3 in Appendix). It is well known that HF theory always overestimates the HOMO-LUMO gap [68]. There is a discontinuity in excitation energies at $\delta r = 0 \text{ \AA}$ for HF and DFT approaches. This is due to the fact that the number of C-C bonds is different for the two oligomers and this affects the excitation energies. Longer chains have lower excitation energies, hence the excitation energies for the 7-bonds OA are larger than those for 9-bonds OA. For CIS calculations, the excitation energies are only slightly smaller (approximately 0.3 eV) for the 9-bonds OA in comparison to the 7-bonds OA.

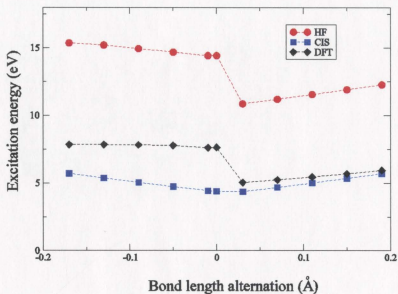


Figure 5.4: Excitation energy as a function of the bond length alternation for 7 ($BLA \leq 0$) and 9 ($BLA > 0$) C-C bonds of OA.

5.2 OLIGOTHIOPHENE (OTH)

5.2.1 Average polarizability per C-C bond vs bond length alternation

From figure 5.5 and table 2.1 (see Appendix), we observe that for the three computational methods α/bond increases as δr increases from -0.17 \AA to

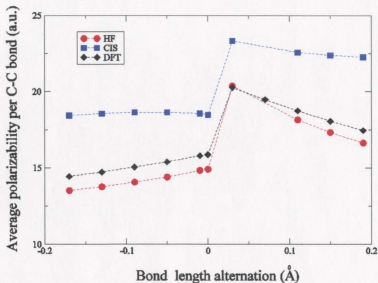


Figure 5.5: Evolution of average polarizability per C-C bond as function of the bond length alternation for the aromatic ($BLA \leq 0$) and quinonoid ($BLA > 0$) structures of OTH .

0 Å and then decreases as δr increases from 0.03 Å to 0.19 Å. All methods show the same trend in α/bond as a function of δr but they differ in magnitude. HF and DFT values for α/bond have shown exactly the same trends and similar magnitudes. CIS results show similar trend in comparison to DFT and HF but the magnitude of the α/bond is greater by a factor ~ 1.3 . For the aromatic structure, the α/bond increases slowly and almost linearly with δr and then decreases rather slowly for the

quinonoid structure but with a steeper slope. In all the methods, α /bond is larger for the quinonoid structure than for the aromatic structure.

For any δr , in all the methods, similar to OA results, we have found the longitudinal component α_{xx} to be the largest, indicating that the charge redistribution in the presence of an electric field is along the chain backbone. The component α_{yy} is the second largest. α_{zz} and α_{xy} are smaller than both α_{xx} and α_{yy} . The other components α_{yz} and α_{xz} are negligible (see table 2.1 in Appendix).

5.2.2 First order hyperpolarizability vs bond length alternation

From figure 5.6 and table 2.2 (see Appendix), it is observed that for the two computational methods, the variation of β_{xxx} and β_{zzz} , as function of δr is very different for the aromatic structure and the quinonoid structure. The coordinate system used for the calculations of β for OTH is similarly defined as for OA (see section 5.1.2). For the aromatic structure, β_{xxx} is the dominant component of $\overset{\text{|||}}{\beta}$ and for the quinonoid structure β_{xxx} and β_{zzz} have similar magnitudes and are the dominant components of $\overset{\text{|||}}{\beta}$. Figure 5.6 shows that β_{xxx} and β_{zzz} are independent of δr for the aromatic structure. For the quinonoid structure, there are some variations of β_{xxx} and β_{zzz} with δr . In addition for the quinonoid structure, β_{xyy} , β_{xzx} and β_{zzz} components also make significant contributions to β .

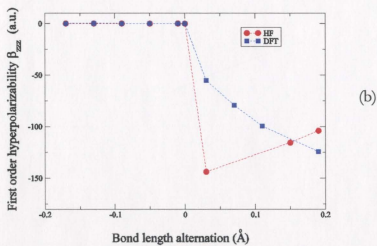
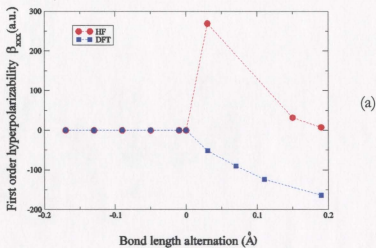


Figure 5.6: Evolution of first order hyperpolarizability (a) β_{xxx} and (b) β_{zzz} as a function of the bond length alternation for the aromatic ($BLA \leq 0$) and quinonoid ($BLA > 0$) structures of OTH.

The other components have very small contributions on β and compared to β_{xxx} and β_{zzz} , those are negligible.

The reason, for which β is significantly larger for the quinonoid isomers, is because the molecules are no longer centro-symmetric when =CH₂ end group was added at one end of the OTH dimer. This was done (as discussed in Chapter 3) in order to have the same number of double bonds in both aromatic and quinonoid isomers.

5.2.3 Excitation Energy vs bond length alternation

From figure 5.7 and table 2.3 (see Appendix), we observe that the three computational methods give excitation energies (ΔE) that decrease as δr increases from - 0.17 Å to 0 Å and then increase as δr increases from 0.03 Å to 0.19 Å. For both the aromatic and quinonoid structures, ΔE decreases as δr tends to zero. Similar to OA results, CIS and DFT give comparable values for the excitation energies whereas HF calculations, for the excitation energies, are larger by a factor of ~ 2.3 (see table 2.3 in Appendix). There is a small discontinuity in excitation energies at $\delta r = 0$ Å for all three methods. The excitation energies for the quinonoid structures are slightly lower than for the aromatic structures.

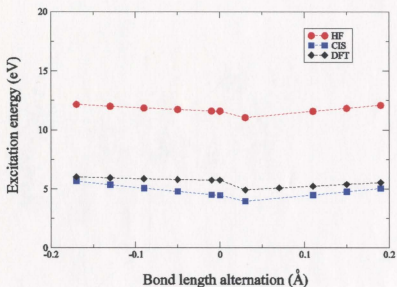


Figure 5.7: Excitation energy as function of the bond length alternation for the aromatic ($BLA \leq 0$) and quinonoid ($BLA > 0$) structures of OTH.

5.3 OLIGOCYCLOPENTADIENE (OCY)

5.3.1 Average polarizability per C-C bond vs bond length alternation

From figure 5.8 and table 3.1 (see Appendix), for the three computational

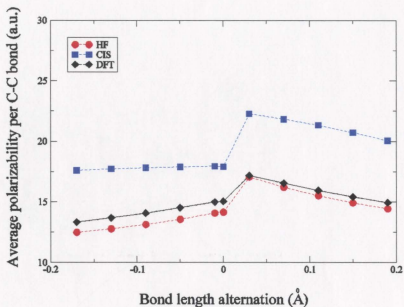


Figure 5.8: Evolution of average polarizability per C-C bond as a function of the bond length alternation for the aromatic ($BLA \leq 0$) and quinonoid ($BLA > 0$) structures of OCY.

methods, we observe that α increases as δr increases from -0.17 \AA to 0 \AA and then decreases as δr increases from 0.03 \AA to 0.19 \AA . The comments that we have made for OTH in section 5.2.1, regarding α/bond , are also applicable to OCY and will not be repeated here. The only difference is the fact that CIS values are greater than HF and DFT values by a factor of ~ 1.3 instead of ~ 2.3 .

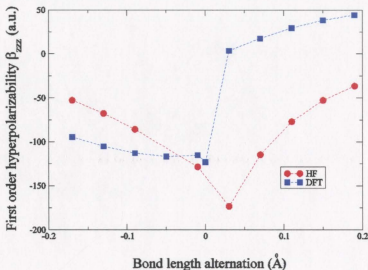


Figure 5.9: Evolution of first order hyperpolarizability β_{zzz} as function of the bond length alternation for the aromatic ($BLA \leq 0$) and quinonoid ($BLA > 0$) structures of OCY.

5.3.2 First order hyperpolarizability vs bond length alternation

From table 3.2 (see Appendix), we can see that for both HF and DFT methods, β_{zzz} is the dominant component of $\vec{\beta}$. β_{zzz} , as function of δr , is

plotted in figure 5.9. Again, Z-Matrix orientation coordinate system is defined as in section 5.1.2. β_{zzz} is larger for the quinonoid structure than for the aromatic structure, for the same reason discussed in section 5.2.2. The other smaller but still significant components of β are β_{xxx} , β_{xxz} and β_{xzz} . As for OA, for OCY, components of β peak around $\delta r = 0 \text{ \AA}$ but not at $\delta r = 0 \text{ \AA}$.

5.3.3 Excitation energy vs bond length alternation

From figure 5.10 and table 3.3 (see Appendix), we observe that the three computational methods show that excitation energies (ΔE) decrease as δr increases from -0.17 \AA to 0 \AA and then increase as δr increases from 0.03 \AA to 0.19 \AA . Similar comments, regarding the trends of the excitation energies as function of δr , made for OTH also apply for OCY. The only difference is that HF values are greater by a factor of ~ 1.9 and ~ 3.3 for DFT and CIS methods respectively (see figure 5.10 and table 3.3 in Appendix).

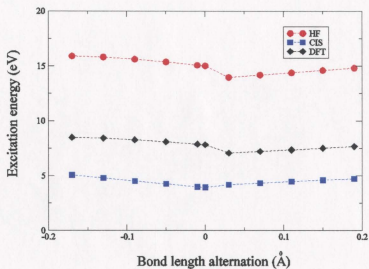


Figure 5.10: Excitation energy as a function of the bond length alternation for the aromatic ($BLA \leq 0$) and quinonoid ($BLA > 0$) structures of OCY.

5.4 OLIGOFULVENE (OFV)

5.4.1 Average polarizability per C-C bond vs bond length alternation

From figure 5.11 and table 4.1 (see Appendix), we observe that for the three computational methods, α/bond increases as δr increases from

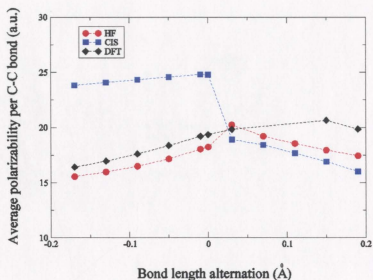


Figure 5.11: Evolution of average polarizability per C-C bond as a function of the bond length alternation for the aromatic ($BLA \leq 0$) and quinonoid ($BLA > 0$) structures of OFV.

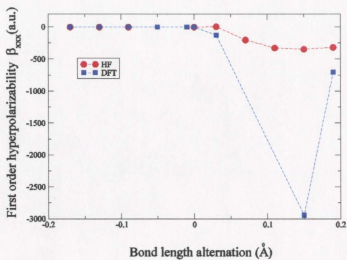
- 0.17 Å to 0 Å and then decreases as δr increases from 0.03 Å to 0.19 Å. OFV shows a similar trend as observed for OTH and OCY (see sections 5.2.1 and 5.3.1) for the aromatic structure. In fact, HF and DFT values for $\alpha/bond$ show similar behavior and magnitude for both the structures (except at $\delta r = 0.15$ Å where DFT result is anomalous). But for CIS there is a drop in the magnitude of $\alpha/bond$ for the quinonoid structure. CIS results for the aromatic structure, in comparison to DFT and HF, is greater by a factor of ~ 1.5 . We suspect that the side groups, located at the tip of

the ring, containing the double bonds in OFV are the main reason for this behavior. As pointed out earlier, the double bonds have significant effects on the polarizability. Hence for OFV, depending on the methods, the aromatic structure is almost or more polarizable than the quinonoid structure.

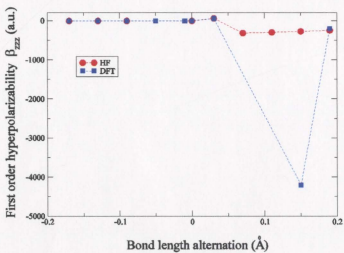
In the coordinate system in which the calculations of α are carried out, y is the direction along the oligomer backbone and x is perpendicular to the xy plane. For any δr , in all the methods, we have found that the longitudinal component α_{yy} is the largest, indicating that the charge redistribution in presence of an electric field is along the chain backbone. The component α_{xx} is also large but α_{zz} and α_{xy} are smaller than α_{xx} and α_{yy} . The other components, α_{yz} and α_{xz} , are negligible (see table 4.1 in Appendix).

5.4.2 First order hyperpolarizability vs bond length alternation

From figure 5.12 and table 4.2 (see Appendix), it can be seen that for the two computational methods, the variation of β_{xxx} and β_{zzz} as function of δr , is very different for the aromatic and the quinonoid structures. The coordinate system used for the calculations of β for OFV is similarly defined as for OA (see section 5.1.2). For both the structures, β_{xxx} is the dominant component of β . β_{zzz} , β_{xxz} and β_{zxx} are also comparable to β_{xxx} (see table 4.2 in Appendix). Figure 5.12 shows that β_{xxx} and β_{zzz} are independent on δr for the aromatic structure.



(a)



(b)

Figure 5.12: Evolution of first order hyperpolarizability (a) β_{xxx} and (b) β_{zzz} as a function of the bond length alternation for the aromatic ($BLA \leq 0$) and quinonoid ($BLA > 0$) structures of OFV.

For the quinonoid structure there are some variations of β_{xxx} and β_{zzz} with δr . In addition, for the quinonoid structure, β_{xyy} and β_{yyz} components make significant contributions to β . The other components, compared to β_{xxx} and β_{zzz} , are negligible. Again larger variations of β for quinonoid structures are due to the fact that oligomers are not centro-symmetric.

5.4.3 Excitation energy vs bond length Alternation

From figure 5.13 and table 4.3 (see Appendix), we observe that the three computational methods give excitation energies (ΔE) that decrease as δr increases from -0.17 \AA to 0 \AA and then increase as δr increases from 0.03 \AA to 0.19 \AA . For both the aromatic and quinonoid structures, ΔE decreases as δr tends to zero, except at $\delta r = 0.03 \text{ \AA}$, where there is a discontinuity for HF and DFT. In all the methods, excitation energies are larger for quinonoid isomers. This is an opposite behavior, in comparison to OA, OTH and OCY (see figures 5.4, 5.7 and 5.10). CIS and DFT methods give comparable values for the excitation energies, whereas HF values for the excitation energies are larger by a factor of ~ 2.3 (see table 4.3 in Appendix). Similar to OTH and OCY, for all the methods we can see the discontinuity in excitation energies at $\delta r = 0 \text{ \AA}$.

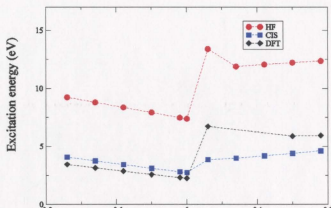


Figure 5.13: Excitation energy as a function of the bond length alternation for the aromatic ($BLA \leq 0$) and quinonoid ($BLA > 0$) structures of OFV.

5.5 OLIGO-DICYANOMETHYLENE CYCLOPENTADITHIOPHENE (OCNTH)

5.5.1 Average polarizability per C-C bond vs bond length alternation

From figure 5.14 and table 5.1 (see in Appendix), for the three computational methods, we observe that α increases as δr increases from

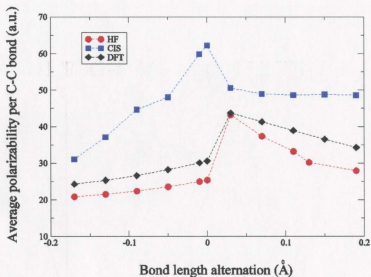


Figure 5.14: Evolution of average polarizability per C-C bond as a function of the bond length alternation for the aromatic ($BLA \leq 0$) and quinonoid ($BLA > 0$) structures of OCNTH.

- 0.17 Å to 0 Å and then decreases as δr increases from 0.03 Å to 0.19 Å. The similar comments that we have made for OTH in section 5.2.1 regarding the trends of α/bond as a function of δr also apply to OCNTH and will not be repeated here. Here we only note that CIS results are greater than HF and DFT values by a factor of ~ 1.3 to ~ 1.5 instead of ~ 1.3 . For any δr , in all the methods, similar to other oligomers studied, we have found that the longitudinal component α_{yy} is the largest, indicating

that the charge redistribution, in the presence of an electric field, is along the chain backbone. The component α_{xx} is comparable to α_{yy} , particularly for the aromatic structure. α_{zz} and α_{xy} are smaller than α_{xx} and α_{yy} . The other components, α_{yz} and α_{xz} , are negligible (see table 5.1 in Appendix).

5.5.2 First order hyperpolarizability vs bond length alternation

From figure 5.15 and table 5.2 (see Appendix), we observe that for the two computational methods, the variation of β_{xxx} and β_{zzz} as function of δr are very different for the aromatic structures and the quinonoid structures. The coordinate system used for the calculations of β for OCNTH is similarly defined as for OA (see section 5.1.2). For the aromatic structures, β_{zzz} is the dominant component of β . And for the quinonoid structures, all the components of β are non-negligible, and among them, β_{xxx} and β_{zzz} are the dominant components of β . Figure 5.15 shows that β_{xxx} and β_{zzz} are roughly independent of δr for the aromatic structures. For the quinonoid structures, because the compound is not centro-symmetric, there are some variations of β_{xxx} and β_{zzz} with δr . In addition, for the quinonoid structures, β_{xxy} , β_{xyy} , β_{yyy} , β_{xxz} , β_{xyz} , β_{yyz} , β_{xzz} and β_{yzz} components make significant contributions to β .

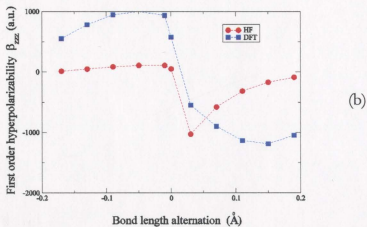
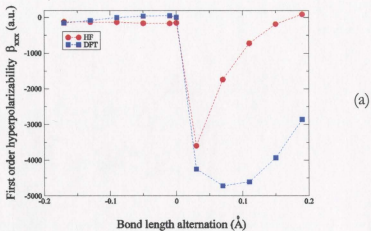


Figure 5.15: Evolution of first order hyperpolarizability (a) β_{xxx} and β_{zzz} as a function of the bond length alternation for the aromatic (BLA \leq 0) and quinonoid (BLA $>$ 0) structures of OCNTH.

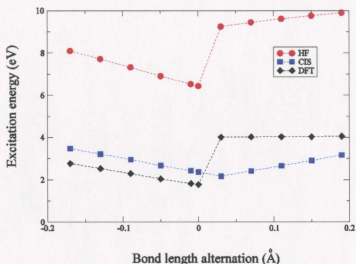


Figure 5.16: Excitation energy as a function of the bond length alternation for the aromatic ($BLA \leq 0$) and quinonoid ($BLA > 0$) structures of OCNTH.

5.5.3 Excitation Energy vs bond length alternation

From figure 5.16 and table 5.3 (see Appendix), we observe that the three computational methods show that excitation energies (ΔE) decrease as δr increases from -0.17 \AA to 0 \AA and then increase as δr increases 0.03 \AA to 0.19 \AA . Similar comments, regarding the trends of the excitation energies as a function of δr , that were made for OFV, apply also for OCNTH. The

only difference is that HF values are greater by a factor of ~ 2.6 and ~ 3.2 for CIS and DFT methods respectively (see figure 5.16 and table 5.3 in Appendix).

Chapter 6

DISCUSSIONS AND CONCLUSIONS

We have studied the dependence of the polarizabilities and the excitation energies on the chain length for the oligomers OTH, OCY, OFV, OCNTH, OCNCY and OCNFV (see Chapter 4). The BLA effects upon α , β and ΔE for the oligomers OTH, OCY, OFV and OCNTH were also investigated (see Chapter 5).

In this chapter we compare the behavior of the different oligomers and summarize the results obtained. Where possible, we compare our results with the previous works. However, comparison with the experiment is limited by the lack of experimental data. In the absence of experimental data, it is difficult to assess the accuracy of the present method. We compare the behavior of the parent oligomers in section 6.1, their cyano derivatives in section 6.2, and the thiophene and its cyano derivative in section 6.3. In section 6.4, we compare our results with the previous works and in section 6.5, we summarize our conclusions.

6.1 Comparison of OTH, OCY and OFV

With the increase of the oligomer length, the polarizabilities and the excitation energies of OTH, OCY and OFV oligomers have increased and decreased respectively. All three have shown the same trend in SOS and CIS methods but the results differ in magnitude (see figures 4.1 and 4.2 in Chapter 4). In both methods, for all oligomers, we can see strong chain length dependence of α for the shorter oligomers and then leveling off for the longer oligomers around 7 to 8 monomers. ΔE also becomes constant (see figures 4.3, 4.4 and 4.5) as the chain length increases in the CIS approach. With the oligomer length α increases in the order of OFV>OCY>OTH and excitation energies decrease OTH>OCY>OFV respectively.

In order to access the magnitude dependence of α on the theoretical method used, we computed, for dimers, the polarizabilities and excitation energies using HF and DFT as well as CIS methods (see figure 6.1 and table 7.1 in Appendix). Calculated CIS polarizabilities and HF excitation energies are the largest for all molecules. HF overestimation of excitation energies is well known and is not unexpected. However, the size of CIS polarizabilities relative to HF and DFT is not so well known.

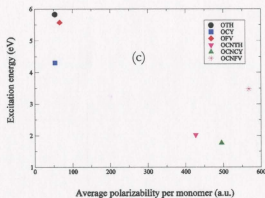
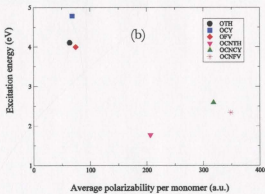
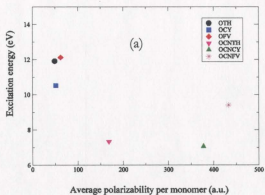


Figure 6.1: Evolution of excitation energy as function of average polarizability per monomer of the dimer molecules in (a) HF, (b) CIS and (c) DFT methods.

In all methods, for OTH, OCY and OFV oligomers, with the increase of BLA, α/bond increases for the aromatic structure and decreases for the quinonoid structure (see figures 5.5, 5.8 and 5.11 in Chapter 5). In HF, CIS and DFT methods, OTH and OCY show a similar trend but differ in magnitude. α/bond is the largest for OFV. In a case of OTH and OCY, the magnitude of α/bond is larger for the quinonoid than for aromatic structure. For OFV, the magnitude of α/bond is larger for the aromatic structure than for quinonoid structure (CIS method). But for HF and DFT methods, the magnitude of α/bond for quinonoid structure is slightly larger than for aromatic structure.

With the increase of BLA, HF and DFT approaches show that β is approximately independent of δr for the aromatic structure but some variation can be seen for the quinonoid structure (see figures 5.6, 5.9 and 5.12). In all cases, β_{xxx} and β_{zzz} are the dominant components of β as the molecules are at an angle in the xz plane (see Chapter 5). As discussed in Chapter 3, the reason for which β exhibits variation for the quinonoid structure is due to the fact that in this case the unit cell is not centrosymmetric. This means that only non centrosymmetric oligomers will give rise to finite first order hyperpolarizability that peaks at finite intermediate δr (not $\delta r = 0 \text{ \AA}$).

From figures 5.7, 5.10 and 5.13, we can see that for all molecules, for both aromatic and quinonoid structures, ΔE decreases as δr tends to zero (for OFV, there is a discontinuity at $\delta r = 0.03 \text{ \AA}$). For OTH and OCY, the

excitation energies of the quinonoid structures are slightly lower than for the aromatic structures but OFV shows the opposite behavior.

6.2 Comparison of OCNTH, OCNCY and OCNFV

In both SOS and CIS methods, with the increase of the oligomer length, the polarizabilities of OCNTH, OCNCY and OCNFV oligomers increase up to tetramers. There is a decrease for seximer in SOS and CIS for OCNTH (see figures 4.1, 4.2, 4.3 and 4.4). Also for OCNTH, with the increase of the oligomer length, in SOS method, we can see that the approximate average polarizability per monomer decreases relative to other oligomers (see figure 4.3). This is not the case for the average SOS and CIS polarizabilities. With the increase of the oligomer length, the increasing order of α is OCNFV > OCNCY > OCNTH. For OCNCY and OCNFV, the excitation energies decrease with the increase of the oligomer length but for OCNTH there is an increase at tetramer (see figures 4.5 and 4.6).

Similar comments, regarding the polarizabilities and the excitation energies, that were made for the dimer molecule for OTH, OCY and OFV in section 6.1 also apply to OCNTH, OCNCY and OCNFV (see table 7.1 in Appendix).

6.3 Comparison of OTH and OCNTH

We find that in all methods, OCNTH has the larger polarizability but the lower excitation energy than OTH (see figures 4.1, 4.2, 4.5 and 4.6). With the increase of the chain length, they show the same trend but with a decrease in polarizability in OCNTH at seximer. We suspect that for larger oligomers α would increase at a similar rate as in OTH (see figures 4.3 and 4.4).

The BLA effects upon α for the three methods are shown in figure 6.2. They show the same trend in α for both structures of OTH and OCNTH but differ in magnitude (by a factor of ~ 1.6 to ~ 2). The longitudinal component of α is the dominant component of α for OTH and OCNTH.

For both OTH and OCNTH, in the two methods, β_{xxx} and β_{zzz} are the dominant components in β (see in tables 2.2 and 5.2 in Appendix). We plot β_{xxx} to show the evolution of β as function of δr (see figure 6.3). Again due to asymmetric structure, the quinonoid structure displays variation of β as function of δr especially for the DFT method (see figure 6.3). ΔE is larger for OTH than OCNTH in all methods (see figure 6.4).

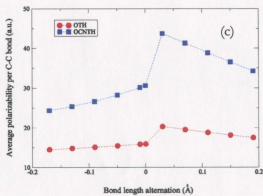
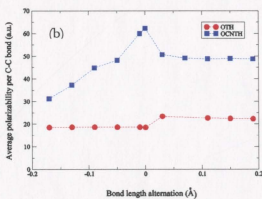
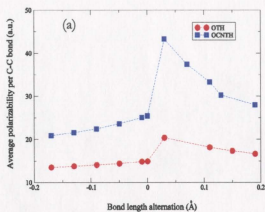


Figure 6.2: Evolution of average polarizability per C – C bond as a function of bond length alternation for the aromatic ($BLA \leq 0$) and quinonoid ($BLA > 0$) structures of OTH and OCNTH in (a) HF, (b) CIS and (c) DFT.

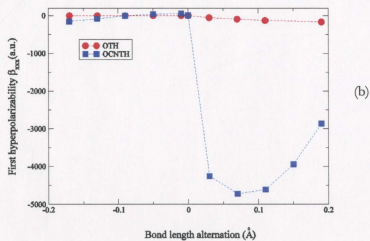
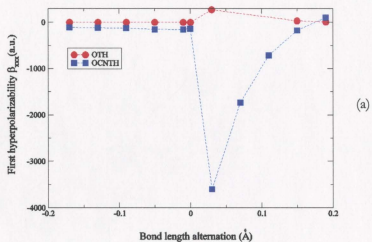


Figure 6.3: Evolution of the first order hyperpolarizability as a function of bond length alternation for the aromatic ($BLA \leq 0$) and quinonoid ($BLA > 0$) structures of OTH and OCNTH in (a) HF and (b) DFT.

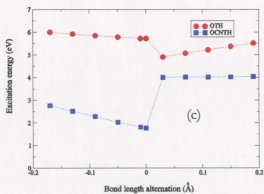
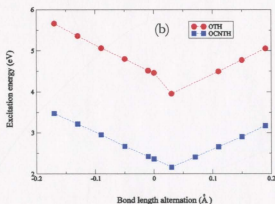
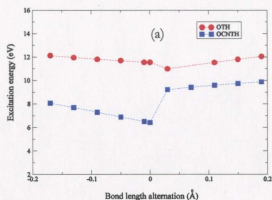


Figure 6.4: Evolution of excitation energy as a function of bond length alternation for the aromatic ($BLA \leq 0$) and quinonoid ($BLA > 0$) structures of OTH and OCNTH in (a) HF, (b) CIS and (c) DFT methods.

6.4 Comparison of our results with the previous works

Table 6.1: Comparison of our calculated data and the experimental data of α/n for OTH. Units are atomic units (a.u.), where 1 a.u. = $1.64877 \times 10^{-41} \text{ C}^2 \text{ m}^2 \text{ J}^{-1}$.

No. of rings (n)	Our calculated result				Calculated	Experimental		
	α/n by SOS	α/n by CIS	α/n by HF	α/n by DFT	α/n^a	α/n^b	α/n^c	α/n^d
1	48.82	48.41			44.5	66.9	66.0	
2	53.24	63.87	48.90	53.62	49.6	84.4		
4	57.82	97.47			59.3	168.7	50.7	23.6
6	58.82	121.27			65.5	506.1		
8	58.53	130.07						

^aReferences 15 and 45.

^bExperimental measurements at $\lambda = 589 \text{ nm}$ in THF solution, reference [38].

^cExperimental measurements at $\lambda = 632.8 \text{ nm}$ in a thin film [38].

^dExperimental measurements at $\lambda = 632.8 \text{ nm}$ in a thin film matrix of

PMMA [37].

In table 6.1, we compare our results with the previous works for OTH. It can be seen from the table that our results in SOS method in gas phase is approximately same as Champagne *et al.* who computed α using coupled and uncoupled Hartree-Fock levels with 3-21G basis set [15]. Our calculated result for a dimer in HF method has good agreement with Champagne *et al.* The calculated α/n in SOS method is fairly good agreement with the result by Zhao *et al.* from the experimental measurements at $\lambda = 632.8$ nm in a thin film [38]. But the experimental measurements at $\lambda = 589$ nm in THF solution by Zhao *et al.* [38] is larger than our calculated results and Champagne *et al.* [15]. This is due to the fact that the THF solvent having larger effect on the polarizabilities [33]. It can be seen from table 6.1 that CIS results overestimate and SOS method gives good agreement with experimental polarizabilities for the longer oligomers. The results in the table indicate that the polarizability is extremely sensitive to the nature and physical state of the chains.

In table 6.2 and 6.3, we compare our calculated CIS excitation energies for OTH, OCY, OFV, OCNTH, OCNCY and OCNFV oligomers with the Chakraborty *et al.* [22, 39]. We have found that there are only few differences between our and Chakraborty *et al.*'s results (these differences are due to the fact that we used the keyword Freq (see in [42, 43, 59]) in our Gaussian calculations).

Table 6.2: Comparison of our calculated CIS excitation energies (in eV) with Chakraborty *et al.* for different oligomer with the method/basis set RCIS/3-21G*.

Oligomer	OTH		OCY		OFV	
	Calculated	^a Ref	Calculated	^b Ref	Calculated	^b Ref
Monomer	5.57	5.57(5.17)	5.36	6.35	6.45	6.46
Dimer	4.10	4.11(3.87)	4.78	4.79	4.00	4.00
Tetramer	3.19	3.19(3.16)	3.36	3.36	3.05	3.05
Seximer	2.91	2.92(2.85)	2.93		2.74	
Octamer	2.83	2.83	2.80	2.81	2.65	2.65
Decamer	2.82	2.82	2.77	2.77		
12-mer		2.82	2.77	2.77		

^aRef: see reference [39] and references within.

^bRef: see reference [22].

Note: experimental values are given in parentheses from ^aRef.

Table 6.3: Comparison of our calculated CIS excitation energies (in eV) with Chakraborty *et al.* the for different oligomers in their most stable configuration with the method/basis set RCIS/3-21G*.

Oligomer	OCNTH		OCNCY		OCNFV	
	Calculated	^a Ref	Calculated	^b Ref	Calculated	^b Ref
Monomer	1.93	1.93	3.58	3.58	3.47	3.47
Dimer	1.78	1.78	2.59	2.59	2.34	2.35
Tetramer	1.98	1.63	2.56	2.57	2.31	2.34
Seximer	2.01	1.99		2.54		2.32

^aRef: see reference [39] and references within.

^bRef: see reference [22].

6.5 Conclusions

From the investigations we find that for a specific molecule, α is larger for larger oligomer length. α has the largest value along the longitudinal direction due to the electron delocalization along the backbone of the molecules. For all, in CIS, HF and DFT methods, we found that the longitudinal component is the largest component in α and increases with the chain length. Paras N. Parsad *et al.* have shown theoretically that the longitudinal polarizability increases rapidly to the number of the repeat units for π -conjugated chain molecules [69]. Hurst *et al.*, in their investigation on the polyene systems via *ab initio* coupled-perturbed Hartree-Fock theory, found that the longitudinal component is the largest in α [27]. Jacquemin *et al.*, in their theoretical study of the longitudinal polarizability and first order hyperpolarizability of polysilaacetylene, have mentioned that the longitudinal components very often dominate the total response [19].

For the parent oligomers, the polarizability per monomer increases smoothly with the oligomer length and then shows an asymptotic behavior with n . Villesuzanne *et al.*, in their study with the π -electron calculations of the polarizabilities in conjugated systems using the finite-field technique, have found the same result [29]. Kirtman *et al.*, in their observation of *ab initio* SCF calculations of the static longitudinal polarizability for polydiacetylene and polybutatriene, have found that the longitudinal

polarizability per number of repeat units n becomes constant when n is sufficiently large [44]. For the parent oligomers we found no saturation of the conjugation up to $n = 7$. Zhao *et al.* [38] also found no saturation of the conjugation up to $n = 6$. Thienpont *et al.* [37] found that the saturation of the polarizability occurs at $n = 7$. For OTH, OCY and OFV we found a strong oligomer length dependence of α/n for $n \leq 7$, that changes into a much weaker, more or less constant for $n > 7$, where the excitation energy becomes constant also. For the cyano derivatives OCNTH, OCNCY and OCNFV, we can not see the leveling off as the saturation regime does not occur if the chains are not long enough. Kirtman *et al.* have mentioned this in their observation [44].

For all oligomers, ΔE decreases with the increase of the oligomer length. Zhao *et al.*, in their observation of thiophene oligomers in THF solutions, found the same result [38]. Thienpont *et al.* observed the same result in their investigation on the saturation of the polarizability of oligothiophenes [37]. The parent oligomers have higher excitation energies and lower α , and cyano derivatives have lower excitation energies and higher α . This result is consistent with Chakraborty *et al.* [22, 39] and Subramanian *et al.* [40].

After investigating the effects of BLA on α , we have found that the end groups and number of double bonds have significant effects on the polarizabilities but single bonds do not have mentionable effects. In HF, CIS and DFT methods; for OA, OTH, OCY, OFV and OCNTH, α/bond

increases with the increase of δr from -0.17 \AA to 0 \AA and then decreases as δr increases from 0.03 \AA to 0.19 \AA . For, OA, α /bond is approximately equal for both the isomers but for OTH, OCY and OCNTH, it is found that the quinonoid structure is more polarizable than the aromatic structure. For OFV, we have found that for CIS method, the aromatic structure is more polarizable than the quinonoid structure but for HF and DFT, it shows the same trend as for OTH, OCY and OCNTH. This trend agrees with Brédas *et al.*, who, in their study for the third-order nonlinear optical response in organic materials, mentioned that the quinonoid geometric structure should be more highly polarizable than the aromatic geometric structure [13].

For all molecules it was found that α /bond increases when δr tends to zero and the largest contribution to α comes from its longitudinal component. Meyers *et al.*, in their investigation on the electric field modulated nonlinear properties of donor-acceptor polyene for 9-(dimethylamino) nona-2,4,6,8-tetraenyl molecule (DAO) using sum over states (SOS) formulation, have shown the variation of α with BLA which is same as what we find for OA [32]. Champagne *et al.* have found the same result in their investigation on the bond length alternation effects on the static electronic polarizability of the polyacetylene chains [18].

Gorman *et al.* have done an investigation of the interrelationships between linear and nonlinear polarizabilities and BLA in conjugated organic molecules (several prototypical macrocyanines) by using the AM1

parameterization in the MOPAC software package [70]. They have shown the variation of α with BLA which is similar to what we have observed.

For OA, in HF and DFT methods, β increases as δr increases from -0.17 Å to 0 Å and decreases as δr increases from 0.03 Å to 0.19 Å. β drops around $\delta r = 0$ Å but not exactly at $\delta r = 0$ Å. The variation of β with δr (see figure 5.3) shows the same trend as Meyers *et al.*, found in their investigation with the 9-(dimethylamino) nona-2,4,6,8-tetraenal molecule (DAO) using sum over states (SOS) formulation [32]. Marder *et al.* in their discussion about the design and synthesis of chromophores and polymers for electro-optic and photorefractive applications, have shown the variation of β as function of BOA for a simple donor-acceptor polyene, $(\text{CH}_3)_2\text{N}-(\text{CH}=\text{CH})_4-\text{CHO}$. It was examined at the semi-empirical 'intermediate neglect of differential overlap-configuration interaction' (INDO-CI) level [71].

Gorman *et al.*, also, in their investigation of the interrelationships between linear and nonlinear polarizabilities and BLA in conjugated organic molecules, have shown the variation of β as function of BLA [70]. They all observed a trend of β with BLA (or BOA) same to what we observe in OA. For OA, from figure 5.3 we can see the shape of the β evolutions as function of δr is first derivative-like with respect to the α evolution (see figure 5.2). For OTH, OCY, OFV and OCNTH, the variation of β as function δr is very different for the aromatic structure and the quinonoid structure. In both HF and DFT methods, for all, β shows some variation with δr for the quinonoid structure in comparison to the aromatic structure

(which, as mentioned before, is due to the fact that the oligomers are no longer centro-symmetric in the quinonoid structures). As first order hyperpolarizability is calculated in the Z-matrix orientation coordinate systems, we found, for OA, OTH, OCY, OFV and OCNTH, the components β_{xxx} and β_{zzz} have the dominant contributions to β . The other components have also a significant effect especially for OCNTH (in quinonoid structure).

In HF, CIS and DFT methods, for OA, OTH, OCY, OFV and OCNTH, we observe that ΔE decreases as δr increases from -0.17 \AA to 0.0 \AA and increases as δr increases from 0.03 \AA to 0.19 \AA . For OA, we found that ΔE is larger for the 7-bond OA than for the 9-bond OA as longer chains have lower excitation energies. For OTH, OCY and OCNTH, in all methods, for both the aromatic and quinonoid structure, ΔE decreases as δr tends to zero. For OTH and OCY, ΔE for aromatic structure is slightly larger than for the quinonoid structure but for OFV and OCNTH, we can see the opposite behavior.

From our observations, we find that calculated CIS polarizabilities are larger than the other methods studied. DFT results are often found to be improved over the Hartree-Fock results. It is also mentioned by Guan *et al.*, in their paper, for comparison of local-density and Hartree-Fock calculations of molecular polarizabilities and hyperpolarizabilities [66]. HF excitation energies are overestimated than CIS and DFT results. Chakraborty *et al.* also found the same result in their observation [22].

From the present study we can therefore obtain the following important conclusions:

- (1) For both SOS and CIS methods, with the increase of the oligomer length, the polarizabilities and the excitation energies of OTH, OCY and OFV oligomers have increased and decreased respectively.
- (2) For OTH, OCY and OFV, the polarizability per monomer becomes constant at the higher oligomer length in both SOS and CIS methods.
- (3) ^{For} In both SOS and CIS methods, with the increase of the oligomer length, the polarizabilities of OCNTH, OCNCY and OCNFV oligomers increase up to tetramers but there is a decrease for seximer in SOS and CIS for OCNTH.
- (4) For OCNCY and OCNFV, the excitation energies decrease with the increase of the oligomer length but for OCNTH there is an increase at tetramer in both methods.
- (5) The cyano ^{derivative} groups have ~~the~~ larger polarizabilities but ~~the~~ lower excitation energies ^{than} ~~its~~ parent oligomers. ^{than} ~~its~~ parent oligomers. ^{in comparison to}
- (6) The longitudinal component of the polarizability has the largest value. That indicates that the charge redistribution in the presence of an electric field is along the chain backbone.
- (7) For all oligomers, we found an inverse relationship between the excitation energies and the polarizabilities.

- (8) The magnitude of the CIS polarizability is larger than the SOS polarizability.
- (9) In HF, CIS and DFT methods, for OA, we observe that α /bond increases for $BLA \leq 0$ and decreases for $BLA > 0$.
- (10) For OA, α /bond has a maximum value at $BLA = 0 \text{ \AA}$ (cyanine limit).
- (11) For both HF and DFT methods, for OA, the first order hyperpolarizability increases for $BLA \leq 0$ and $BLA > 0$, but there is a drop near $BLA = 0 \text{ \AA}$.
- (12) For OA, HF and DFT methods show the same trend for the first order hyperpolarizability but give different magnitudes for β .
- (13) For OTH, OCY, OFV and OCNTH, in all methods, the quinonoid structure ($BLA > 0$) is more polarizable than the aromatic structure ($BLA \leq 0$) (except for OFV in CIS method).
- (14) For all systems, in HF and DFT methods, β is approximately independent of BLA for the aromatic structure.
- (15) For all, β is significantly larger for the quinonoid structure ($BLA > 0$). The molecules are no longer centro-symmetric when $=CH_2$ end group was added at one end of the OTH, OCY, OFV and OCNTH oligomers and hence β is finite.

- (16) In the three computational methods, excitation energies decrease for $BLA \leq 0$ and increase for $BLA > 0$ (except for OFV).
- (17) For both the aromatic and quinonoid structures, ΔE decreases as BLA tends to zero.
- (18) In all methods, with the increase of BLA , the cyano substituted OCNTH has larger polarizabilities and lower excitation energies than the parent oligomer OTH.

6.6 Future work

From our observation we have found that the end groups have a significant effect on the polarizabilities. To eliminate the need for end groups, it would be useful to use the periodic boundary condition (PBC option in Gaussian 03). It is therefore suggested that in future this study should be done with the PBC option.

BIBLIOGRAPHY

- [1] Cited from the website, <http://www.designinsite.dk/htmsider/m1328.htm>, Date: 04/08/2004.
- [2] Cited from the website, <http://www.mmrc.caltech.edu/colin/science/past/PhD/html-thesis/node8.html>, Date: 19/07/2004.
- [3] P.Otto. *International Journal of quantum chemistry*, Vol. 52, 353-364, 1994, and reference therein.
- [4] Bernard Kirtman and Muhammad Hasan, *J. Chem. Phys.* 96 (1), 1 January 1992.
- [5] G.R Hutchison, Yu-Jun Zhao, B. Delley, A.J. Freeman, M.A. Ratner and T.J. Marks, *Physical review* B68, 035204 (2003) and references therein.
- [6] Arnold C. Alguno, Wilfredo C. Chung, Rolando V. Bantaculo, Hitoshi Miyata, Edgar W. Ignacio and Angelina M. Bacala, "A density functional calculation of polypyrrole and polythiophene energy band gaps". Cited from the website: physics.msuiit.edu.ph/spvm/papers/2001/alguno.pdf.
- [7] Sung Y. Hong, Si J. Kwon and Shi C. Kim, *J. Chem. Phys.* 103(5), 1871-1877, 1995 and references therein.
- [8] J. L. Brédas, *Science*, Vol. 263, 28 January 1994
- [9] N.C. Billingham, P.D.Calvert, Y. Kurimura, I.M.Papisov and A.A. Litmanovich., *Advances in Polymer Science* 90@Springer-Verlag Berlin

- Heidelberg 1989 and reference therein.
- [10] D. Beljonne, Z. Shuai and J. L. Brédas, *J. Chem.Phys.* 98 (11), 1 June 1993
- [11] Terje A. Skotheim, Ronald L. Elsenbaumer and John R. Reynolds, Handbook of conducting Polymers, second edition, chapter 1copyright@1998 by Marcel Dekker Inc.
- [12] S. Grigoras, G.C. Lie, T.J.Barton, S. Ijadi-Maghsoodi, Y Pang and J. Shinar, Z.V. Vardeny, K.S. Wong, and S.G.Han, *Synthetic Metals*, 49-50 (1992) 293-304.
- [13] J. L. Brédas, C. A dant, P. Tackx and A. Persoons. *Chem. Rev.* Vol. 94, 243-278, 1994.
- [14] Jean-Marie André and Joseph Delhalle, *Chem.Rev.*1991, 91, 843-865.
- [15] B. Champagne, D. H. Mosley and J.-M André. *J.Chem.Phys.* 100(3), 1 February 1994.
- [16] Z. An and K.Y.Wong, *Journal of Chemical Physics*, Vol. 119, No. 2, 8 July 2003.
- [17] Bernard Kirtman, *International Journal of quantum chemistry*, Vol. 43, 147-158, 1992.
- [18] Benoît Champagne and Eric A. Perpète, *International Journal of Quantum Chemistry*, Vol. 75, 441-447, 1999.
- [19] Denis Jacquemin, Eric A. Perpète and Jean-Marie

- André, *Journal of Chemical Physics*, Vol. 120, No. 21, 1 June 2004.
- [20] George Maroulis and Ajit J. Thakkar, *J.Chem.Phys.* 95(12), 9060, 15 December 1991.
- [21] Shi-yi Liu and Clifford E. Dykstra. *J.Phys.Chem.* 91, No.7, page 1749, 1987.
- [22] D. Chakraborty and J.B.Lagowski, *Polymer* 45 (2004) 1331-1344.
- [23] Edet F. Archibong and Ajit J. Thakkar. *J.Chem.Phys.* 98(10), 15 May 1993.
- [24] Erik K. Dalskov, Jens Oddershede and David M. Bishop, *J.Chem. Phys.*108(5), 1February 1998.
- [25] Joseph L. Toto, Teresa Tangredi Toto, Celso P. de Melo, Bernard Kirtman and K. Robins, *J. Chem. Phys.* Vol. 104, No. 21, 1 June 1996.
- [26] P. Chopra, L. Carlacci, H. F.King and P.N.Prasad, *J.Phys.Chem.* 93, 7120 (1989).
- [27] G.J.B. Hurst, M.Dupuis and E. Clementi , *J.Chem.Phys.* 89,385, 1988.
- [28] L. Ducasse, A. Villesuzanne, J. Hoarau and A. Fritsch, *J. Chem .Phys.* 97(12), 15 December 1992.
- [29] A. Villesuzanne, J. Hoarau , L. Ducasse, L. Olmedo and P. Hourquebie, *J. Chem. Phys.* 96(1), 1 January 1992.
- [30] C.P. de Melo and R. Silbey, *J. Chem. Phys.* 88 (4), page 2558, 15 February 1988.

- [31] C. P. de Melo and R. Silbey, *J. Chem. Phys.* 88 (4), page 2567, 15 February 1988.
- [32] F. Meyers, S. R. Marder, B.M. Pierce, and J.L. Brédas. *J. Am. Chem. Soc.* 116, 10703-10714, 1994.
- [33] Yi Luo, Patrick Norman, Peter Macak and Hans Ågren, *J. Chem. Phys.* Vol.111, No. 21, 1 December 1999.
- [34] Benoît Champagne, Denis Jacquemin, Jean-Marie André and Bernard Kirtman; *J. Phys. Chem. A* 1997, 101, 3158-3165.
- [35] F.C. Grozema, R. Telesca, H.T. Jonkman, L.D.A. Siebbeles, and J.G. Snijders, *J. Chem. Phys.* Vol. 115, No. 21, 1 December 2001.
- [36] Alan Hinchliffe and Humberto J. Soscu'n Machado, *Int. J. Mol. Sci.* 2000, 1, 39-48.
- [37] H.Thienpont, G.L.J.A Rikken and E.W.Meijer, *Physical review letters*. Vol. 65, No. 17, 22 October 1990.
- [38] M.T.Zhao, B.P. Singh and P.N. Prasad, *J. Chem. Phys.* 89(9), 5535, 1988.
- [39] D. Chakraborty and J. B. Lagowski, *J. Chem. Phys.* Vol. 115, No. 2, 8 July 2001.
- [40] Hamsa Subramanian and Jolanta B. Logowski, *International Journal of Quantum Chemistry*, Vol. 66, 229-240 (1998).
- [41] Jing Ma, Shuhua Li and Yuansheng Jiang,

Macromolecules, Vol. 35, No.

3, 1109-1115, 2002.

- [42] M.J.Frisch, G.W.Trucks, Æleen Frisch, H.B. Schlegel, P.M.W.Gill, B.G. Johnson, M.A.Robb, J. R. Cheeseman, T. A. Keith, G.A. Petersson, J. A. Montgomery, K. Raghavachari, M. A. Al-Laham, V.G.Zakrzewsk, J. V. Ortiz, J. B. Foresman, J. Cioslowski, B. B. Stefanov, A. Nanavakkara, M. Challacombe, C. Y. Peng, P. Y. Alaya, W. Chen, M. W. Wong, J. L. Andres, E. S. Replogle, R. Gomperts, R. L. Martin, D. J. Fox, J. S. Binkley, J. A. Defrees, J. Baker, J. P. Stewart, M. Head-Gordon, C. Gonzalez and J. A. Pople, Gaussian 94, Revision A. 1, Gaussian, Inc., Pittsburgh, PA, 1995.
- [43] M.J.Frisch, G.W.Trucks, Æleen Frisch, H. B. Schlegel, G. E. Scuseria, M. A. Robb, J. R. Cheeseman, V. G. Zakrzewski, J. A. Montgomery, R. E. Stratmann, J. C. Burant, S. Dapprich, J. M. Millam, A. D. Daniels, K. N. Kudin, M. C. Strain, O. Farkas, J. Tomasi, V. Barone, M. Cossi, R. Cammi, B. Mennucci, C. Pomelli, C. Adamo, S. Clifford, J. Ochterski, G. A. Petersson, P. Y. Alaya, Q. Cui, K. Morokuma, D. K. Malick, A. D. Rabuck, K. Raghavachari, J. B. Foresman, J. Cioslowski, J. V. Ortiz, B. B. Stefanov, G. Liu, A. Liashenko, P. Piskorz, I. Komaromi, R. Gomperts, R. L. Martin, D. J. Fox, T. Keith, M. A. Al-

- Laham, C. Y. Peng, A. Nanavakkara, C. Gonzalez, M. Challacombe, P. M. W. Gill, B. G. Johnson, W. Chen, M. W. Wong, J. L. Andres, M. Head-Gordon, E. S. Replogle and J. A. Pople, Gaussian 98, Revision A. 1, Gaussian, Inc., Pittsburgh, PA, 1998.
- [44] Bernard Kirtman and Muhammad Hasan, *Chemical Physics Letters*, Vol. 157, No. 1, 2; 28 April 1989.
- [45] Keith D. Bonin and Vitaly V. Kresin. "Electric-Dipole Polarizabilities of Atoms, Molecules and Clusters" Chapter 1, 3; Page 1 and 62, Copyright@1997 by World Scientific Publishing Co. Pte. Ltd.
- [46] P. W. Atkins and R. S. Friedman, *Molecular Quantum Mechanics*, pp382-388, Third edition, Oxford University Press, 1997.
- [47] P. W. Atkins and R. S. Friedman, *Molecular Quantum Mechanics*, pp183, Third edition, Oxford University Press, 1997.
- [48] J. M. Thijssen, *Computational Physics*, Cambridge University Press, 1999, pp 45-47.
- [49] Keith D. Bonin and Vitaly V. Kresin. "Electric - Dipole Polarizabilities of Atoms, Molecules and Clusters" Chapter 4, Copyright@1997 by World Scientific Publishing Co. Pte. Ltd.
- [50] Neil W. Ashcroft and N. David Mermin, *Solid State Physics*, Chapter 17,

- Page329, Copyright @ 1976
by Harcourt, Inc.
- [51] Attila Szabo and Neil S. Ostlund, *Modern Quantum Chemistry, Introduction to Advanced Electronic Structure Theory*, First edition, Revised; First published by Macmillan Publishing Co., Inc. @1982, page127.
- [52] Warren J. Hehre, Leo Random, Paul v.R.Schleyer and John A. Pople, *Ab Initio Molecular Orbital theory*; A Wiley-Interscience Publication, Copyright @1986 by John Wiley & Sons, Inc.; Chapter 4, page 64.
- [53] G.G.Hall, Proc. R. Soc. (London) A205, 541(1951).
- [54] C. C. J. Roothan, Rev. Mod. Phys. 23, 69 (1951).
- [55] S. F. Boys, Proc. R. Soc. (London) A200, 542(1950).
- [56] David C. Young, *Computational Chemistry, A Practical Guide for Applying Techniques to Real-World Problems*, Copyright @2001 by John Wiley & Sons, Inc., page 23-24,216-217.
- [57] Warren J. Hehre, Leo Random, Paul v.R.Schleyer and John A. Pople, *Ab Initio Molecular Orbital theory*; A Wiley-Interscience Publication, Copyright @1986 by John Wiley & Sons, Inc.; Chapter 2, page 32-34.
- [58] P. Hohenberg, W. Kohn, Phys.Rev.B 136 (1964) 864.

- [59] M.J.Frisch, G.W.Trucks, Eelen Frisch, H.B. Schlegel, G.E.Scuseria, M. A. Robb, J. R. Cheeseman, J. A. Montgomery, Jr. T. Vreven, K. N. Kudin, J. C. Burant, J. M. Millam, S. S. Iyengar, J. Tomasi, V. Barone, B. Mennucci, M. Cossi, G. Scalmani, N. Rega, G. A. Petersson, H. Nakatsuji, M. Hada, M. Ehara, K. Toyota, R. Fukuda, J. Hasegawa, M. Ishida, T. Nakajima, Y. Honda, O. Kitao, H. Nakai, M. Klene, X. Li, J. E. Knox, H.P. Hratchian, J. B. Cross, C. Adamo, J. Jaramillo, R. Gomperts, R. E. Stratmann, O. Yazyev, A. J. Austin, R. Cammi, C. Pomelli, J. W. Ochterski, P. Y. Ayala, K. Morokuma, G. A. Voth, P. Salvador, J. J. Dannenberg, V. G. Zakrzewski, S. Dapprich, A. D. Daniels, M. C. Strain, O. Farkas, D. K. Malick, A. D. Rabuck, K. Raghavachari, J. B. Foresman, J. V. Ortiz, Q. Cui, A. G. Baboul, S. Clifford, J. Ciosolwski, B. B Stefanov, G. Liu, A. Liashenko, P. Piskorz, I. Komaromi, R. L. Martin, D. J. Fox, T. Keith, M. A. Al-Laham, C. Y. Peng, A. Nanavakkara, M. Challacombe, P. M. W. Gill, B. G. Johnson, W. Chen, M. W. Wong, C. Gonzalez, and J. A. Pople, Gaussian 03, Revision A. 1, Gaussian, Inc., Pittsburgh, PA, 2003.
- [60] K. Raghavachari and J. A. Pople, *International Journal of Quantum Chemistry*, Vol. 20, page 1067, 1981.
- [61] R. Krishnan, H. B. Schlegel and J. A. Pople, *J. Chem.*

Phys., Vol. 72, No. 8, 15
April 1980.

edition, Copyright © 1993,
1995-96 Gaussian, Inc.

- [62] David C. Young, *Computational Chemistry, A Practical Guide for Applying Techniques to Real-World Problems*, Copyright ©2001 by John Wiley & Sons, Inc., page 336-337, 349-350.
- [63] A. B. Nielsen and A. J. Holder, Gaussian User's Reference, Carnegie Office Park, Building 6, Pittsburgh, PA 15106, USA, 1997, Version 1.0.
- [64] E. R. Davidson and D. Feller, *Chem. Rev.* 86, 681-696, 1986.
- [65] James B. Foresman and Eileen Frisch, *Exploring chemistry with electronic structure methods*, Second
- [66] Jingang Guan, Patrick Duffy, Jonathan T. Carter and Delano P. Chong, Kim C. Casida, Mark E. Casida and Michael Wrinn, *J. Chem. Phys.* 98 (6), 15 March 1993.
- [67] J. B. Lagowski and Z. Gong, Personal Communications, Department of Physics and Physical Oceanography, Memorial University of Newfoundland, E-mail address:
jolantal@physics.mun.ca
- [68] Cheol Ho Choi, Miklos Kertesz and Alfred Karpfen, *J. Chem. Phys.* 107 (17), 1 November 1997.

- [69] Paras N. Prasad, Eric Perrin, and Marek Samoc, *J. Chem. Phys.*, Vol. 91 (4), 15 August 1989.
- [70] Christopher B. Gorman and Seth R. Marder, *Proc. Natl. Acad. Sci. USA* Vol. 90, pp. 11297 - 11301, December 1993.
- [71] Seth R. Marder, Bernard Kippelen, Alex K. -Y Jen & Nasser Peyghambarian; *Nature*, Vol. 388, 28 August 1997.

APPENDIX
SUPPLEMENTARY DATA

Table 1.1 : Average polarizability per C-C bond with the change of the bond length of OA for parital optimization in three different methods.

Molecule	Method	Bond length (Å)	Polarizability (a.u.)						Average polarizability (a.u.)	Average Polarizability per C-C bond α/bond (a.u.)
			α_{xx}	α_{yy}	α_{zz}	α_{xy}	α_{yz}	α_{xz}		
OA	HF	(1.38, 1.43)	274.038	71.624	20.215	-36.722	0.002	0.003	121.959	17.422
	CIS		462.999	70.243	20.710	-16.525	0.001	0.002	184.650	26.378
	DFT		282.975	70.843	21.707	-20.483	0.000	0.000	125.175	17.882
	HF	(1.36, 1.45)	246.979	71.318	20.245	-33.966	0.000	0.004	112.847	16.121
	CIS		453.251	69.754	20.726	-14.928	0.000	0.000	181.243	25.891
	DFT		260.449	70.807	21.713	-20.176	0.000	-0.001	117.656	16.808
	HF	(1.34, 1.47)	224.677	71.032	20.281	31.473	0.001	-0.026	105.330	15.047
	CIS		442.872	69.350	20.747	13.833	0.001	-0.064	177.656	25.379
	DFT		239.854	70.777	21.726	19.754	0.001	-0.003	110.785	15.826
	HF	(1.32, 1.49)	206.453	70.756	20.322	-29.212	0.002	-0.010	99.177	14.168
	CIS		431.628	69.006	20.773	-13.060	0.001	-0.007	173.802	24.828
	DFT		221.452	70.748	21.744	-19.245	0.000	-0.002	104.648	14.949
	HF	(1.40, 1.40)	313.742	71.81	20.173	-40.112	0.003	0.006	135.241	19.320
	CIS		471.860	70.788	20.678	-19.269	0.003	0.004	187.775	26.825
	DFT		310.924	70.771	21.687	-20.506	0.000	0.000	134.460	19.208
	HF	(1.40, 1.41)	306.947	71.942	20.192	-39.753	0.002	0.006	133.027	19.000
	CIS		473.249	70.827	20.690	-18.845	0.002	0.004	188.258	26.894
	DFT		306.966	70.881	21.708	-20.647	0.000	0.000	133.185	19.026
	HF	(1.42, 1.39)	357.266	89.182	39.564	-44.440	-0.001	0.008	162.004	18.004
	CIS		593.747	87.323	40.344	-23.598	0.000	0.013	240.471	26.716
	DFT		386.337	88.217	41.202	22.993	0.000	-0.012	171.918	19.102
	HF	(1.44, 1.37)	318.366	88.847	39.653	-40.615	0.001	-0.006	148.942	16.549
	CIS		576.281	86.814	40.397	-21.957	0.000	-0.012	234.497	26.055
	DFT		352.164	88.219	41.255	22.824	0.000	-0.011	160.546	17.838
	HF	(1.46, 1.35)	287.159	88.542	39.751	37.201	-0.001	-0.006	138.484	15.387
	CIS		559.336	86.422	40.462	20.857	0.000	-0.011	228.740	25.415
	DFT		321.256	88.230	41.323	22.408	0.000	-0.010	150.269	16.696
	HF	(1.48, 1.33)	262.218	88.261	39.855	34.144	-0.001	-0.005	130.111	14.456
	CIS		542.114	86.120	40.535	20.042	0.000	-0.011	222.923	24.769
	DFT		294.027	88.247	41.401	21.800	0.000	-0.009	141.225	15.691
HF	(1.50, 1.31)	242.269	88.006	39.963	31.401	-0.001	-0.005	123.412	13.712	
CIS		524.308	85.885	40.616	19.366	0.000	-0.011	216.933	24.103	
DFT		270.563	88.267	41.487	21.067	0.000	-0.010	133.439	14.826	

Table 1.2 : First order hyperpolarizability with the change of the bond length of OA for partial optimization in two different methods.

Molecule	Method	Bond length (Å)	First order hyperpolarizability $\times 10^{-3}$ (a.u.)									
			β_{xxx}	β_{xxy}	β_{xyy}	β_{yyy}	β_{xxz}	β_{yyz}	β_{yzy}	β_{zzz}	β_{yzz}	β_{zzz}
OA	HF	(1.38,	-0.0619	5.4671	0.0055	-0.8163	-0.0416	24.1066	0.019	0.5596	28.9517	1.6331
	DFT	1.43)										
	HF	(1.36,	2.3682	17.6056	-0.0252	-11.1609	4.3544	30.4985	0.1387	5.3285	120.9197	1.537
	DFT	1.45)	78.034	3.5511	1.5249	-1.6375	181.112	11.2348	-2.655	444.88	26.351	880.43
	HF	(1.34,	-1.6621	3.9373	0.479	8.8906	-2.8889	-56.733	0.4802	-2.532	-128.497	1.903
	DFT	1.47)	51.804	-2.635	1.6101	1.021	135.509	-7.749	-2.622	365.72	-13.526	731.29
	HF	(1.32,	-2.0351	2.5268	0.3722	-106.438	-5.9552	346.0802	-0.629	0.8158	1146.5	16.043
	DFT	1.49)	24.226	36.727	1.648	-14.257	85.759	65.552	-2.531	276.01	90.604	561.15
	HF	(1.40,	-0.809	30.5767	0.0024	-4.4427	-2.1912	71.6274	0.0557	-3.4662	66.5561	-3.175
	DFT	1.40)	120.446	3.2125	1.679	-0.6528	257.106	8.6334	-2.673	584.09	17.173	1148.1
	HF	(1.40,	-0.9238	26.0514	0.0022	-4.4966	-2.383	64.1766	0.0577	-3.809	66.942	-3.659
	DFT	1.41)	123.435	2.8125	1.632	-0.668	262.978	8.1064	-2.739	597.56	16.503	1172.9
	HF	(1.42,										
	DFT	1.39)	-231.10	0.55707	4.058	5.2739	-461.48	1.3121	56.449	-1047.13	-3.176	-2589.39

CONTINUED (SEE THE NEXT PAGE)

Table 1.2 (continued): First order hyperpolarizability with the change of the bond length of OA for parital optimization in two different methods.

Molecule	Method	Bond length (Å)	First order hyperpolarizability $\times 10^{-3}$ (a.u.)									
			β_{xxx}	β_{xxy}	β_{xyy}	β_{yyy}	β_{xxz}	β_{xyx}	β_{yyz}	β_{xzz}	β_{yzz}	β_{zzz}
OA	HF	(1.44,	-111.39	-8.8682	-11.2768	5.8468	-108.84	-2.4958	-7.280	-113.47	-0.889	-203.1643
	DFT	1.37)	-166.54	0.8236	-33.89	-5.058	-305.28	1.2109	-14.223	-677.67	-4.0501	-1909.89
	HF	(1.46,	-93.600	-8.8368	-15.3315	6.7157	-72.1182	-1.8158	-10.07	-42.153	-0.7654	-88.393
	DFT	1.35)	-136.84	1.1131	-36.273	5.171	-243.67	1.1446	-16.817	-550.728	-5.180	-1687.02
	HF	(1.48,	-73.540	-8.525	-19.404	7.3191	-37.166	-1.2379	-13.239	19.918	-0.614	3.962
	DFT	1.33)	-119.036	1.603	-45.260	5.577	-200.04	1.2784	-22.93	-462.55	-6.487	-1618.54
	HF	(1.50,	-56.037	-8.431	-23.629	8.219	-8.940	-0.7454	-16.79	68.274	-0.558	70.62
	DFT	1.31)	-93.430	2.164	-56.904	6.753	-138.33	1.639	-31.212	-329.6	-8.4018	-1460.6

Table 1.3 : Excitation energy and average polarizability per C-C bond of OA for partial optimization in three different methods.

Molecule	Method	Bond length (Å)	Excitation energy (eV)	Average Polarizability (a.u.)	Average Polarizability per C-C bond α /bond (a.u.)
OA	HF	(1.38, 1.43)	14.690	121.959	17.422
	CIS		4.725	184.650	26.378
	DFT		7.772	125.175	17.882
	HF	(1.36, 1.45)	14.951	112.847	16.121
	CIS		5.039	181.243	25.891
	DFT		7.812	117.656	16.808
	HF	(1.34, 1.47)	15.218	105.330	15.047
	CIS		5.364	177.656	25.379
	DFT		7.831	110.785	15.826
	HF	(1.32, 1.49)	15.369	99.177	14.168
	CIS		5.698	173.802	24.828
	DFT		7.841	104.648	14.949
	HF	(1.40, 1.40)	14.438	135.241	19.320
	CIS		4.374	187.775	26.825
	DFT		7.625	134.460	19.208
	HF	(1.40, 1.41)	14.433	133.027	19.000
	CIS		4.424	188.258	26.894
	DFT		7.611	133.185	19.026
	HF	(1.42, 1.39)	10.873	162.004	18.004
	CIS		4.351	240.471	26.716
	DFT		5.038	171.918	19.102
	HF	(1.44, 1.37)	11.215	148.942	16.549
	CIS		4.672	234.497	26.055
	DFT		5.239	160.546	17.838
	HF	(1.46, 1.35)	11.567	138.484	15.387
	CIS		5.005	228.740	25.415
	DFT		5.455	150.269	16.696
	HF	(1.48, 1.33)	11.927	130.111	14.456
	CIS		5.346	222.923	24.769
	DFT		5.687	141.225	15.691
HF	(1.50, 1.31)	12.294	123.412	13.712	
CIS		5.695	216.933	24.103	
DFT		5.933	133.439	14.826	

Table 2.1 : Average polarizability per C-C bond with the change of the bond length of OTH for partial optimization in three different methods.

Molecule	Method	Bond length (Å)	Polarizability (a.u.)						Average polarizability (a.u.)	Average Polarizability per C-C bond α /bond (a.u.)
			α_{xx}	α_{yy}	α_{zz}	α_{xy}	α_{yz}	α_{zx}		
OTH	HF	(1.38, 1.43)	155.006	112.791	34.576	7.274	0.000	0.001	100.809	14.401
	CIS		247.452	108.731	35.103	4.228	0.000	0.001	130.428	18.6325
	DFT		173.176	114.142	35.761	6.879	0.000	0.002	107.693	15.3847
	HF	(1.36, 1.45)	148.025	112.902	34.592	-7.271	0.000	0.001	98.506	14.072
	CIS		247.259	109.003	35.015	-5.463	0.000	0.000	130.425	18.6321
	DFT		166.153	114.232	35.774	-6.873	0.000	0.001	105.386	15.0551
	HF	(1.34, 1.47)	141.820	112.78	34.613	-7.113	0.000	0.000	96.4043	13.772
	CIS		245.708	109.160	35.022	-6.596	0.000	0.000	129.9633	18.5661
	DFT		159.383	114.195	35.788	-6.745	0.001	0.001	103.122	14.7317
	HF	(1.32, 1.49)	136.749	112.509	34.637	-6.885	0.000	0.000	94.631	13.518
	CIS		242.829	109.279	35.036	-7.535	0.000	0.000	129.048	18.4354
	DFT		153.379	114.071	35.806	-6.569	0.000	0.000	101.085	14.4407
	HF	(1.40, 1.40)	166.471	112.213	34.559	7.113	0.000	0.002	104.414	14.916
	CIS		244.939	108.122	35.013	2.511	0.000	0.000	129.358	18.4797
	DFT		183.472	113.739	35.746	6.743	0.000	0.002	110.985	15.855
	HF	(1.40, 1.41)	164.48	112.616	34.569	7.221	0.000	0.000	103.888	14.841
	CIS		246.400	108.523	35.023	2.797	0.000	-0.001	129.952	18.5688
	DFT		181.842	114.051	35.761	6.851	0.000	0.000	110.551	15.793
	HF	(1.42, 1.39)	344.411	101.732	42.774	-4.856	0.002	-0.008	162.972	20.3715
	CIS		391.308	125.366	43.033	-20.518	0.003	-0.009	186.569	23.3211
	DFT		330.175	111.915	44.279	-6.198	-0.012	-0.114	162.123	20.2653
	HF	(1.44, 1.37)								
	CIS									
	DFT		312.40	110.784	44.296	-4.846	-0.013	-0.110	155.8266	19.4783
	HF	(1.46, 1.35)	292.471	100.290	42.859	1.9370	-0.004	0.020	145.2066	18.150
	CIS		371.051	127.736	43.046	19.145	-0.002	0.029	180.611	22.576
	DFT		295.790	109.746	44.32	-3.628	-0.014	-0.105	149.952	18.744
	HF	(1.48, 1.33)	273.04	99.823	42.909	0.967	0.008	-0.005	138.5906	17.323
	CIS		365.114	128.991	43.062	18.15	0.009	-0.007	179.055	22.3818
	DFT		280.341	108.814	44.351	2.531	-0.003	0.081	144.502	18.0627
HF	(1.50, 1.31)	256.804	99.511	42.964	0.229	0.013	0.015	133.093	16.6366	
CIS		360.766	130.335	43.084	16.948	0.019	0.054	178.06166	22.2577	
DFT		266.244	108.06	44.389	1.577	0.001	0.077	139.5649	17.4455	

Table 2.2 : First order hyperpolarizability with the change of the bond length of OTH for partial optimization in two different methods.

Molecule	Method	Bond length (Å)	First order hyperpolarizability (a.u.)									
			β_{xxx}	β_{xyx}	β_{yyx}	β_{yyy}	β_{xzz}	β_{yzz}	β_{zyz}	β_{zzx}	β_{zzy}	β_{zzz}
OTH	HF	(1.38,	-0.415838	-0.004131	-0.009571	0.0002454	-0.85331	-0.000973	-0.010739	-0.2734561	-0.001385	-0.14242
	DFT	1.43)	-0.33729	0.004611	-0.013381	0.0001452	-0.804861	-0.869	-0.014430	-0.402258	-0.007804	-0.23220
	HF	(1.36,	0.103598	-0.003420	-0.000709	-0.000168	0.067649	0.0000941	-0.000918	-0.005121	0.001145	-0.062442
	DFT	1.45)	-0.050403	-0.001479	-0.002732	-0.002730	-0.051113	0.003362	-0.001115	-0.037537	0.008469	-0.022468
	HF	(1.34,	0.103812	-0.000794	-0.001078	-0.000282	0.077733	-0.000216	-0.000991	-0.0032714	0.001039	-0.070099
	DFT	1.47)	-0.51666	-0.025424	-0.005766	-0.012958	-0.34339	0.01656	-0.001946	-0.117996	0.05716	0.007392
	HF	(1.32,	0.078297	-0.000978	-0.001022	-0.000309	0.069007	0.004318	-0.000788	-0.001326	0.001762	-0.06292
	DFT	1.49)	-0.016720	-0.000204	-0.003836	-0.002049	-0.027237	0.002429	-0.001561	-0.027663	0.006791	-0.023667
	HF	(1.40,	0.13268	0.012676	-0.000407	0.002541	0.065312	0.008319	-0.000924	-0.020362	-0.002927	-0.087857
	DFT	1.40)	-0.098205	0.038873	-0.001812	0.021221	-0.083062	0.031854	-0.001096	-0.044914	-0.040792	-0.020666
	HF	(1.40,	0.072635	-0.002012	-0.000179	0.001690	0.03532	0.004926	-0.000532	-0.011729	0.002390	-0.052901
	DFT	1.41)	0.00478	0.005109	-0.001233	0.003521	-0.024687	0.007017	-0.000909	-0.032518	-0.002453	-0.037847
	HF	(1.42,	269.01268	0.403254	45.24042	-0.14190	95.590	0.554900	17.42654	-74.21126	0.687876	-143.4822
	DFT	1.39)	-51.78966	0.207425	50.989.07	-0.04527	106.29302	0.136012	19.04757	8.3496460	0.151413	-55.03214
	HF	(1.44,										
	DFT	1.37)	-90.27124	0.163813	48.395187	-0.03820	57.549334	0.117220	18.27993	-26.18041	0.126377	-79.16066

CONTINUED (SEE THE NEXT PAGE)

Table 2.2 : First order hyperpolarizability with the change of the bond length of OTH for partial optimization in two different methods.

Molecule	Method	Bond length (Å)	First order hyperpolarizability (a.u.)									
			β_{xxx}	β_{xxy}	β_{xyy}	β_{yyy}	β_{xxx}	β_{yyz}	β_{yyz}	β_{zzz}	β_{zzz}	
OTH	HF	(1.46,										
	DFT	1.35)	-123.908	-0.000631	46.23630	-0.03342	13.27959	0.044548	17.69011	-56.94398	0.054344	-99.50449
	HF	(1.48,	31.94617	-0.606232	39.65689	0.15000	-19.6915	-0.554100	15.5715	-94.64082	-0.657472	-115.2517
	DFT	1.33)										
	HF	(1.50,	7.71839	-0.776237	38.461708	-0.104937	-27.6758	-0.946386	15.25289	-89.17677	-0.899348	-103.7968
	DFT	1.31)	-163.8167	-0.596160	42.860066	-0.133653	-50.54585	-0.409307	16.88400	-99.40929	-3152450	-124.2581

Table 2.3 : Excitation energy and average polarizability per C-C bond of OTH for parital optimization in three different methods.

Molecule	Method	Bond length (Å)	Excitation energy (eV)	Average Polarizability (a.u.)	Average Polarizability per C-C bond α /bond (a.u.)
OTH	HF	(1.38, 1.43)	11.720	100.809	14.401
	CIS		4.800	130.428	18.632
	DFT		5.802	107.693	15.384
	HF	(1.36, 1.45)	11.844	98.506	14.072
	CIS		5.064	130.425	18.632
	DFT		5.861	105.386	15.055
	HF	(1.34, 1.47)	11.992	96.404	13.772
	CIS		5.357	129.963	18.566
	DFT		5.935	103.122	14.731
	HF	(1.32, 1.49)	12.152	94.631	13.518
	CIS		5.660	129.048	18.435
	DFT		6.020	101.085	14.440
	HF	(1.40, 1.40)	11.579	104.414	14.916
	CIS		4.461	129.358	18.479
	DFT		5.7424	110.985	15.855
	HF	(1.40, 1.41)	11.587	103.888	14.841
	CIS		4.517	129.982	18.568
	DFT		5.7421	110.551	15.793
	HF	(1.42, 1.39)	11.0312	162.972	20.371
	CIS		3.959	186.569	23.321
	DFT		4.913	162.123	20.265
	HF	(1.44, 1.37)			
	CIS				
	DFT		5.086	155.826	19.478
	HF	(1.46, 1.35)	11.568	145.206	18.150
	CIS		4.497	180.611	22.576
	DFT		5.231	149.952	18.744
HF	(1.48, 1.33)	11.824	138.590	17.323	
CIS		4.774	179.055	22.381	
DFT		5.381	144.502	18.062	
HF	(1.50, 1.31)	12.080	133.093	16.636	
CIS		5.055	178.061	22.257	
DFT		5.536	139.564	17.445	

Table 3.1: Average polarizability per C-C bond with the change of the bond length of OCY for partial optimization in three different methods.

Molecule	Method	Bond length (Å)	Polarizability (a.u.)						Average polarizability (a.u.)	Average Polarizability per C-C bond α /bond (a.u.)
			α_{xx}	α_{yy}	α_{zz}	α_{xy}	α_{yz}	α_{zx}		
OCY	HF	(1.38, 1.43)	145.32	102.60	36.895	-10.306	0.000	0.000	94.94	13.5628
	CIS		236.21	101.74	37.671	6.636	0.000	0.000	125.209	17.887
	DFT		164.68	101.79	38.302	-6.475	0.001	-0.001	101.59	14.512
	HF	(1.36, 1.45)	136.76	102.08	36.915	-10.003	0.000	0.000	91.916	13.130
	CIS		235.36	101.06	37.673	5.994	0.000	0.000	124.6976	17.813
	DFT		155.83	101.42	38.322	-6.690	0.001	0.000	98.527	14.075
	HF	(1.34, 1.47)	129.72	101.53	36.937	9.640	0.000	0.000	89.399	12.771
	CIS		233.99	100.42	37.682	-5.311	0.000	0.000	124.031	17.718
	DFT		147.85	101.07	38.344	-6.773	0.002	0.001	95.756	13.679
	HF	(1.32, 1.49)	124.01	100.98	36.96	-9.245	0.000	0.000	87.32	12.474
	CIS		231.99	99.83	37.698	4.631	0.000	0.000	123.174	17.596
	DFT		140.80	100.72	38.369	-6.759	0.003	0.002	93.2996	13.328
	HF	(1.40, 1.40)	157.53	102.89	36.857	10.417	0.000	0.000	99.092	14.156
	CIS		235.99	102.37	37.665	7.451	0.000	0.000	125.343	17.906
	DFT		175.67	101.98	38.261	-5.924	0.001	-0.002	105.303	15.043
	HF	(1.40, 1.41)	155.75	103.08	36.881	10.504	0.000	0.000	98.5723	14.081
	CIS		236.88	102.45	37.676	-7.202	0.000	0.000	125.668	17.952
	DFT		174.30	102.14	38.289	-6.094	0.001	-0.002	104.910	14.987
	HF	(1.42, 1.39)	270.16	94.29	44.750	-8.260	0.012	0.016	136.402	17.050
	CIS		377.85	111.60	45.259	11.510	0.034	0.034	178.237	22.279
	DFT		263.55	102.10	46.407	2.423	-0.026	-0.099	137.356	17.169
	HF	(1.44, 1.37)	250.54	93.77	44.769	-8.567	0.003	-0.010	129.694	16.2117
	CIS		365.97	112.74	45.283	10.949	0.002	-0.021	174.6683	21.833
	DFT		248.98	101.39	46.401	3.106	-0.022	-0.100	132.2576	16.532
	HF	(1.46, 1.35)	234.10	93.35	44.792	-8.741	0.004	-0.012	124.081	15.510
	CIS		352.57	113.78	45.323	9.754	0.007	-0.008	170.557	21.319
	DFT		235.52	100.73	46.402	3.714	-0.024	-0.095	127.553	15.944
	HF	(1.48, 1.33)	220.30	93.03	44.818	-8.799	0.005	-0.010	119.3866	14.923
	CIS		337.37	114.64	45.383	8.021	0.009	0.002	165.798	20.724
	DFT		223.36	100.13	46.407	4.229	-0.019	-0.086	123.30	15.412
	HF	(1.50, 1.31)	208.72	92.83	44.847	8.756	0.002	0.009	115.468	14.433
	CIS		320.49	115.29	45.464	-5.950	0.003	0.012	160.416	20.052
	DFT		212.54	99.61	46.417	4.641	-0.021	-0.126	119.5246	14.940

Table 3.2 : First order hyperpolarizability with the change of the bond length of OCY for partial optimization in two different methods.

Molecule	Method	Bond length (Å)	First order hyperpolarizability (a.u.)										
			β_{xxx}	β_{xyx}	β_{yyx}	β_{yyy}	β_{xxy}	β_{yyz}	β_{yzy}	β_{zxx}	β_{zyz}	β_{zzz}	
OCY	HF	(1.38,											
	DFT	1.43)	-13.72940	0.0023588	-0.624063	-0.003974	1.688955	0.0010303	-0.479112	-20.537221	-0.000953	-116.7531	
	HF	(1.36,	-11.01938	0.0008562	-0.405520	-0.002071	1.464408	0.0007191	-0.786081	-17.174721	0.000400	-85.83452	
	DFT	1.45)	-13.88003	0.002559	-0.720425	-0.003703	0.846185	0.0013384	0.066535	-21.688152	-0.000660	-112.9904	
	HF	(1.34,	-11.27958	-0.001292	-0.464865	0.002627	0.803020	-0.000849	-0.449244	-14.058337	0.000205	-67.81401	
	DFT	1.47)	-13.89799	0.0036248	-0.870091	-0.004683	0.438753	0.0019554	0.649788	-21.888213	-0.000728	-105.1119	
	HF	(1.32,	-11.25293	0.005072	-0.557177	-0.007004	0.631652	0.0032561	-0.100047	-11.166644	-0.000809	-52.73433	
	DFT	1.49)	-13.77835	0.0072847	-1.063052	-0.010841	0.424189	0.0019684	1.240788	-21.277700	0.001655	-94.63153	
	HF	(1.40,											
	DFT	1.40)	-13.86890	0.0019758	-0.648555	-0.004339	4.061786	0.000291	-1.049541	-17.442253	-0.001861	-123.0272	
	HF	(1.40,	-8.874517	-0.0001941	-0.3821103	-0.000121	5.5497023	-0.000423	-1.336021	-22.886830	0.000725	-128.4561	
	DFT	1.41)	-13.42711	0.0021102	0.5885831	-0.004263	2.9884481	0.0005188	-0.953481	-18.484151	-0.001511	-115.3733	
	HF	(1.42,	-19.59298	0.4099187	9.158205	-0.321386	46.147803	0.5488989	-46.02452	112.37730	-0.320105	-173.3955	
	DFT	1.39)	-22.41096	-0.0841532	8.5469709	0.079973	37.831157	-0.114451	-48.66171	62.725831	-0.110804	3.532881	
	HF	(1.44,	-21.96393	-0.0145086	8.9312241	0.056264	39.442261	-0.040031	-45.42648	97.401915	-0.133835	-114.5208	
	DFT	1.37)	-22.80365	-0.0954132	8.2624754	0.110804	38.7649	-0.269640	-48.11448	73.6705087	-0.236159	17.70467	
	HF	(1.46,	-23.7575	-0.0208435	8.64121	0.052730	33.707	0.07535	-45.03603	83.129787	-0.094208	-77.19522	
	DFT	1.35)	-23.47351	-0.0941307	7.9178375	0.082194	38.456839	-0.173294	-47.75830	80.118423	-0.096391	29.55753	

CONTINUED (SEE THE NEXT PAGE)

Table 3.2 : First order hyperpolarizability with the change of the bond length of OCY for parital optimization in two different methods.

Molecule	Method	Bond length (Å)	First order hyperpolarizability (a.u.)									
			β_{xxx}	β_{xxy}	β_{xyy}	β_{yyy}	β_{xxz}	β_{xyz}	β_{yyz}	β_{zzz}	β_{zzz}	
	HF	(1.48,	-25.08030	0.0237906	8.302652	-0.02554	28.904483	0.1719136	-44.81725	70.102802	0.001257	-52.80701
	DFT	1.33)	-24.37288	-0.103691	7.5243936	0.039870	37.010820	-0.182269	-47.59370	82.353351	0.110232	38.40507
	HF	(1.50,	-26.01085	0.0322651	7.9263128	-0.080440	24.956674	0.045377	-44.74479	58.572077	0.136499	-36.5664
	DFT	1.31)	-25.43760	-0.323731	7.1041778	0.462790	34.602931	-0.522106	-47.61327	81.026266	-0.835959	44.28176

Table 3.3 : Excitation energy and average polarizability per C-C bond of OCY for parital optimization in three different methods.

Molecule	Method	Bond length (Å)	Excitation energy (eV)	Average Polarizability (a.u.)	Average Polarizability per C-C bond α /bond (a.u.)
OCY	HF	(1.38, 1.43)	15.364	94.940	13.562
	CIS		4.249	125.209	17.887
	DFT		8.073	101.590	14.512
	HF	(1.36, 1.45)	15.616	91.916	13.130
	CIS		4.518	124.697	17.813
	DFT		8.266	98.527	14.075
	HF	(1.34, 1.47)	15.802	89.399	12.771
	CIS		4.792	124.031	17.718
	DFT		8.412	95.756	13.679
	HF	(1.32, 1.49)	15.901	87.320	12.474
	CIS		5.069	123.174	17.596
	DFT		8.486	93.299	13.328
	HF	(1.40, 1.40)	15.004	99.092	14.156
	CIS		3.943	125.343	17.906
	DFT		7.814	105.303	15.043
	HF	(1.40, 1.41)	15.067	98.572	14.081
	CIS		3.987	125.668	17.952
	DFT		7.859	104.910	14.987
	HF	(1.42, 1.39)	13.964	136.402	17.050
	CIS		4.1827	178.237	22.279
	DFT		7.057	137.356	17.169
	HF	(1.44, 1.37)	14.174	129.694	16.211
	CIS		4.333	174.668	21.833
	DFT		7.196	132.257	16.532
	HF	(1.46, 1.35)	14.385	124.081	15.510
	CIS		4.475	170.557	21.319
	DFT		7.342	127.553	15.944
	HF	(1.48, 1.33)	14.598	119.386	14.923
	CIS		4.607	165.798	20.724
	DFT		7.496	123.30	15.412
HF	(1.50, 1.31)	14.816	115.468	14.433	
CIS		4.724	160.416	20.052	
DFT		7.657	119.524	14.940	

Table 4.1 : Average polarizability per C-C bond with the change of the bond length of OFV for partial optimization in three different methods.

Molecule	Method	Bond length (Å)	Polarizability (a.u.)					Average polarizability (a.u.)	Average Polarizability per C-C bond α /bond (a.u.)	
			α_{xx}	α_{yy}	α_{zz}	α_{xy}	α_{yz}			α_{xz}
OFV	HF	(1.38, 1.43)	164.63	167.84	27.95	2.153	0.000	0.000	120.139	17.162
	CIS		219.07	268.78	28.20	-60.945	0.000	0.000	172.017	24.573
	DFT		160.09	195.74	29.86	7.477	0.000	0.000	128.562	18.366
	HF	(1.36, 1.45)	162.96	155.35	28.01	4.925	0.000	0.000	115.435	16.490
	CIS		218.51	264.09	28.24	-58.051	0.000	0.000	170.279	24.326
	DFT		158.44	181.26	29.89	3.615	0.000	0.000	123.194	17.599
	HF	(1.34, 1.47)	161.35	145.92	28.07	6.789	0.000	0.000	111.78	15.968
	CIS		218.57	258.81	28.28	-55.153	0.000	0.000	168.552	24.079
	DFT		156.97	169.12	29.92	0.682	0.000	0.000	118.67	16.952
	HF	(1.32, 1.49)	159.77	138.79	28.13	8.019	0.000	0.000	108.895	15.556
	CIS		219.24	252.90	28.32	-52.209	0.000	0.000	166.820	23.831
	DFT		155.59	159.07	29.96	1.546	0.000	0.000	114.871	16.410
	HF	(1.40, 1.40)	166.39	188.73	27.88	-3.444	0.000	0.000	127.668	18.238
	CIS		219.56	272.96	28.16	-64.338	0.000	0.000	173.559	24.794
	DFT		161.93	214.90	29.81	13.473	0.000	0.000	135.544	19.363
	HF	(1.40, 1.41)	166.45	184.51	27.90	-1.937	0.000	0.000	126.289	18.041
	CIS		219.89	272.92	28.17	-63.57	0.000	0.000	173.66	24.808
	DFT		161.87	211.60	29.83	12.032	0.000	0.000	134.433	19.204
	HF	(1.42, 1.39)	129.59	307.03	49.16	-4.957	-4.119	-1.305	161.928	20.241
	CIS		181.08	232.17	40.36	62.134	0.000	0.000	151.204	18.900
	DFT		136.32	289.32	50.36	-1.631	-3.191	-1.431	158.664	19.83
	HF	(1.44, 1.37)	173.36	242.06	45.60	58.020	0.000	0.000	153.675	19.209
	CIS		178.46	224.04	39.59	58.332	0.000	0.000	147.364	18.420
	DFT									
	HF	(1.46, 1.35)	169.99	229.29	45.59	52.705	0.000	0.000	148.286	18.535
	CIS		174.12	212.87	37.06	52.774	0.000	0.000	141.35	17.668
	DFT									
	HF	(1.48, 1.33)	166.98	218.09	45.61	47.908	0.000	0.000	143.561	17.945
	CIS		170.17	203.21	32.30	47.75	0.000	0.000	135.226	16.903
	DFT		199.33	250.47	45.77	73.856	0.542	-0.078	165.19	20.64
HF	(1.50, 1.31)	164.39	208.46	45.71	43.667	0.000	0.000	139.519	17.439	
CIS		166.69	195.02	22.43	43.342	0.000	0.000	128.047	16.005	
DFT		192.60	237.90	45.73	66.129	0.561	-0.104	158.742	19.842	

Table 4.2 : First order hyperpolarizability with the change of
the bond length of OFV for partial optimization in two different methods.

Molecule	Method	Bond length (Å)	First order hyperpolarizability (a.u.)									
			β_{xxx}	β_{xxy}	β_{yyx}	β_{yyy}	β_{xxz}	β_{yyz}	β_{zzx}	β_{yzz}	β_{zzz}	
OFV	HF	(1.38,										
	DFT	1.43)	1.6810941	-0.0000007	0.015027	0.0	1.19787	-0.0000007	-0.0115861	0.5596539	0.0000009	0.043043
	HF	(1.36,	-0.0148585	0.00	-0.0003413	0.00	-0.019708	0.00	-0.0001912	0.0108415	0.0	0.0147281
	DFT	1.45)	0.0830006	-0.0000002	-0.0005822	0.0	0.0478299	0.0000003	-0.0004356	0.0081078	0.0000005	0.019533
	HF	(1.34,	-0.008713	0.00	-0.0003026	0.00	-0.0124315	0.00	-0.000125	0.0051499	0.00	0.004413
	DFT	1.47)	-0.0056805	-0.0000009	-0.0000188	0.0	-0.0306443	0.0000001	-0.0003474	-0.0317623	0.0000005	-0.019181
	HF	(1.32,	-0.0505359	0.0	0.0000487	0.0	-0.0281297	0.0	-0.000029	0.0152499	0.0	0.011959
	DFT	1.49)	-0.0405879	0.0000009	-0.0000792	0.0	-0.0328646	0.0000004	-0.0003672	-0.0307678	0.0000012	0.000139
	HF	(1.40,	-0.129516	0.0	0.0002162	0.0	-0.0575469	0.0	-0.0000694	-0.0438272	0.0	0.002524
	DFT	1.40)	0.0315403	0.0000003	-0.0000286	0.0	0.0036363	-0.0000001	-0.0006421	0.0224894	0.0000013	0.016154
	HF	(1.40,										
	DFT	1.41)	0.0825094	0.0000003	-0.000071	0.0	0.0309799	0.0	-0.0007386	-0.0140174	0.0000012	0.023781
	HF	(1.42,	7.07894	-61.272978	35.676801	-24.480031	355.48671	-43.24028	23.95028	189.99125	-20.01589	64.98539
	DFT	1.39)	-125.9446	-79.81033	47.5654	-24.94661	254.1611	-32.4348	25.26960	144.739	-2.80799	56.9246
	HF	(1.44,	-202.3243	-0.0000088	47.323569	-0.0000033	514.74804	-0.0000008	50.608152	-48.8094669	-0.0000011	-311.6520
	DFT	1.37)										
HF	(1.46,	-326.5486	-0.0000144	74.95313	-0.0000066	388.96619	-0.0000086	68.699723	-50.156464	0.0000003	-293.3326	
DFT	1.35)											

CONTINUED (SEE THE NEXT PAGE)

Table 4.2 : First order hyperpolarizability with the change of the bond length of OFV for partial optimization in two different methods.

Molecule	Method	Bond length (Å)	First order hyperpolarizability (a.u.)									
			β_{xxx}	β_{xxy}	β_{xyy}	β_{yyy}	β_{xxz}	β_{xyx}	β_{yyz}	β_{xzz}	β_{yzz}	β_{zzz}
	HF	(1.48,	-346.16955	-0.0000055	124.206239	-0.000009	310.089	-0.0000035	100.179451	-41.1223778	0.0000029	-269.4529
	DFT	1.33)	-2943.1568	-99.5082	-98.49911	0.0	-4052.56	-18.129	124.968	-4240.5308	25.277	-4202.179
	HF	(1.50,	-319.4472	-0.0000023	222.08931	-0.0000161	260.446145	0.0000003	161.047034	-27.177010	0.0000046	-242.5823
	DFT	1.31)	-708.285	-0.0010455	-185.4948	0.0	142.0139	0.0002177	73.9118	-61.786	0.0011139	-197.253

Table 4.3 : Excitation energy and average polarizability per C-C bond of OFV for partial optimization in three different methods.

Molecule	Method	Bond length (Å)	Excitation energy (eV)	Average Polarizability (a.u.)	Average Polarizability per C-C bond α /bond (a.u.)
OFV	HF	(1.38, 1.43)	7.913	120.139	17.162
	CIS		3.112	172.017	24.573
	DFT		2.575	128.562	18.366
	HF	(1.36, 1.45)	8.352	115.435	16.490
	CIS		3.431	170.279	24.325
	DFT		2.859	123.194	17.599
	HF	(1.34, 1.47)	8.787	111.780	15.968
	CIS		3.752	168.552	24.078
	DFT		3.146	118.670	16.952
	HF	(1.32, 1.49)	9.218	108.895	15.556
	CIS		4.081	166.820	23.831
	DFT		3.439	114.871	16.410
	HF	(1.40, 1.40)	7.379	127.668	18.238
	CIS		2.757	173.559	24.794
	DFT		2.255	135.544	19.363
	HF	(1.40, 1.41)	7.469	126.289	18.041
	CIS		2.813	173.660	24.808
	DFT		2.307	134.433	19.204
	HF	(1.42, 1.39)	13.376	161.928	20.241
	CIS		3.860	151.204	18.900
	DFT		6.722	158.664	19.830
	HF	(1.44, 1.37)	11.867	153.675	19.209
	CIS		3.986	147.364	18.420
	DFT				
HF	(1.46, 1.35)	12.042	148.286	18.535	
CIS		4.191	141.350	17.668	
DFT					
HF	(1.48, 1.33)	12.203	143.561	17.945	
CIS		4.404	135.226	16.903	
DFT		5.880	165.190	20.640	
HF	(1.50, 1.31)	12.348	139.519	17.439	
CIS		4.621	128.047	16.005	
DFT		5.925	158.742	19.842	

Table 5.1 : Average polarizability per C-C bond with the change of the bond length of OCNTH for partial optimization in three different methods.

Molecule	Method	Bond length (Å)	Polarizability (a.u.)						Average polarizability (a.u.)	Average Polarizability per C-C bond α/bond (a.u.)
			α_{xx}	α_{yy}	α_{zz}	α_{xy}	α_{yz}	α_{xz}		
	HF	(1.38, 1.43)	410.32	562.32	91.09	-18.20	0.000	0.000	354.573	23.638
	CIS		715.70	1357.11	90.00	-418.57	0.000	0.000	721.127	48.075
	DFT		438.49	736.81	94.08	-11.46	0.000	-0.001	423.125	28.208
	HF	(1.36, 1.45)	403.25	516.30	91.23	-18.73	0.000	0.000	336.925	22.461
	CIS		724.43	1196.65	91.12	-381.77	0.000	0.000	670.732	44.715
	DFT		432.61	668.98	94.21	10.84	0.000	0.001	398.597	26.573
	HF	(1.34, 1.47)	397.38	482.84	91.36	19.18	0.000	0.000	323.860	21.590
	CIS		635.74	947.11	91.24	244.63	0.000	0.000	558.047	37.203
	DFT		427.68	616.99	94.32	10.80	-0.001	0.001	379.663	25.310
	HF	(1.32, 1.49)	391.57	457.57	91.50	19.14	0.000	0.000	313.549	20.903
	CIS		541.17	768.21	91.36	131.76	0.000	0.000	466.914	31.128
	DFT		422.67	575.61	94.44	10.86	-0.001	0.001	364.24	24.282
	HF	(1.40, 1.40)	415.31	639.38	90.94	15.54	0.000	0.000	381.876	25.458
	CIS		816.27	1890.83	90.89	651.94	0.000	0.000	932.659	62.177
	DFT		442.38	840.25	93.96	13.95	0.000	-0.001	458.86	30.590
	HF	(1.40, 1.41)	415.28	622.31	91.00	17.67	0.000	0.000	376.197	25.079
	CIS		814.83	1785.93	90.94	623.00	0.000	0.000	897.229	59.815
	DFT		442.11	817.80	94.02	-11.99	0.000	-0.001	451.308	30.087
	HF	(1.42, 1.39)	397.12	1581.56	98.90	156.35	-0.002	0.005	692.525	43.282
	CIS		546.39	1782.54	98.80	-46.26	-0.004	0.007	809.244	50.577
	DFT		450.60	1545.57	102.20	106.66	-0.035	-0.135	699.454	43.716
	HF	(1.44, 1.37)	386.71	1311.51	98.99	-126.92	-0.002	0.004	599.0693	37.441
	CIS		564.70	1689.30	98.85	6.61	-0.002	0.002	784.286	49.017
	DFT		441.62	1439.12	102.25	96.20	-0.028	-0.104	660.996	41.312
	HF	(1.46, 1.35)	378.33	1120.91	99.10	106.23	0.001	0.000	532.776	33.299
	CIS		588.63	1649.01	98.92	-55.19	0.002	-0.003	778.854	48.678
	DFT		432.96	1330.88	102.33	86.99	-0.031	-0.115	622.054	38.878
	HF	(1.48, 1.33)	371.44	982.70	99.22	91.14	0.001	-0.003	484.451	30.278
	CIS		616.55	1629.65	98.10	-99.35	0.005	-0.010	781.702	48.856
	DFT		424.81	1225.07	102.42	79.05	-0.031	-0.110	584.432	36.527
	HF	(1.50, 1.31)	365.72	879.82	99.34	79.71	0.000	-0.006	448.292	28.018
	CIS		641.39	1594.00	99.13	-127.24	0.008	-0.015	778.176	48.636
	DFT		417.25	1125.17	102.52	72.21	-0.031	-0.104	548.314	34.269

Table 5.2 : First order hyperpolarizability with the change of the bond length of OCNTH for parital optimization in two different methods.

Molecule	Method	Bond length (Å)	First order hyperpolarizability (a.u.)									
			β_{xxx}	β_{xyx}	β_{yyx}	β_{yyy}	β_{xxy}	β_{yyz}	β_{yzy}	β_{zxx}	β_{zyz}	β_{zzz}
OCNTH	HF	(1.38,	-149.65489	0.0	-0.8945015	0.0	15.6323879	0.0	0.1676686	63.4837669	0.0	112.6577
	DFT	1.43)	41.0684	0.0000163	-0.4001222	0.0	249.123994	0.0000124	0.1054605	535.179046	0.0000056	1001.9854
	HF	(1.36,	-121.9438	0.0	-0.664377	0.0	-6.3611722	0.0	0.2863883	70.9124488	0.0	90.108660
	DFT	1.45)	-1.7394302	0.000114	-0.179637	0.0	202.4355	0.0000892	0.2495569	521.01305	0.0000387	948.243621
	HF	(1.34,	-115.58663	0.0	-0.545698	0.0	-34.550713	0.0	0.4280968	51.4257032	0.0	52.649527
	DFT	1.47)	-79.020335	0.0000026	-0.1116479	0.0	98.0058663	0.0000257	0.4190879	401.570320	0.0000135	783.706167
	HF	(1.32,	-106.96697	0.0	-0.4094936	0.0	-57.896607	0.0	0.5852877	34.27468	0.0	16.992937
	DFT	1.49)	-148.11316	0.0000017	0.0131457	0.0	-8.3413	0.0000042	0.6039665	253.4865	0.0000154	553.3542
	HF	(1.40,	-134.26106	0.0	-0.7237307	0.0	-1.9659413	0.0	0.1002313	-2.7177084	0.0	55.223656
	DFT	1.40)	8.9047547	-0.0003244	-0.337018	0.0	97.328116	-0.0005117	-0.0115833	224.9568	-0.0006842	577.62137
	HF	(1.40,	-150.35535	0.0	-0.8180438	0.0	17.9698703	0.0	0.1227833	54.4594618	0.0	113.190392
	DFT	1.41)	57.6277	0.0000275	-0.361349	0.0	230.9520	0.0000438	0.0439088	482.0342	0.0000831	939.4926
	HF	(1.42,	-3596.3202	-2253.7615	-876.63929	245.8670	-2647.212	-1304.9705	-105.91445	-1762.0542	-539.4675	-1023.5080
	DFT	1.39)	-4250.6252	-1862.4720	-321.2335	921.550	-2627.544	-810.647	529.8407	-1441.909	39.2907	-549.7665
	HF	(1.44,	-1730.2278	-1184.6752	-507.20520	-105.1627	-1327.0832	-702.43896	-68.08313	-920.5925	-303.9486	-575.8667
	DFT	1.37)	-4720.3363	-2274.0367	-688.7602	-600.747	-3054.6017	-1189.2566	196.09285	-1830.245	-303.92219	-899.5987
	HF	(1.46,	-710.8551	-565.344	-285.979	27.0808	-583.9177	-348.9874	-41.8235	-437.3958	-162.9361	-314.1950
	DFT	1.35)	-4606.834	-2424.1889	-984.18497	239.51657	-3101.3464	-1426.0412	-138.05395	-1989.3577	-596.5400	-1134.2816

CONTINUED (SEE THE NEXT PAGE)

Table 5.2 : First order hyperpolarizability with the change of the bond length of OCNTH for partial optimization in two different methods.

Molecule	Method	Bond length (Å)	First order hyperpolarizability (a.u.)									
			β_{xxx}	β_{xxy}	β_{xyy}	β_{yyy}	β_{xxz}	β_{yyz}	β_{yzz}	β_{zzz}		
	HF	(1.48,	-172.470	-215.4581	-159.0133	-17.64427	-177.40964	-148.30755	-27.05878	-168.124615	-82.78336	-166.58355
	DFT	1.33)	-3935.5445	-2247.507	-1106.4284	-52.97030	-2756.0961	-1442.4529	-367.2335	-1877.7582	-746.4393	-1186.8663
	HF	(1.50,	101.5239	-20.72833	-87.26394	-42.1364	39.5380998	-36.220931	-18.564979	-21.060380	-37.746226	-84.52505
	DFT	1.31)	-2855.507	-1786.3755	-1034.7123	-219.2841	-2090.8731	-1237.9166	-448.834	-1516.53038	-726.4190	-1046.084

Table 5.3 : Excitation energy and average polarizability per C-C bond of OCNTH for partial optimization in three different methods.

Molecule	Method	Bond length (Å)	Excitation energy (eV)	Polarizability (a.u.)	Average Polarizability per C-C bond α /bond (a.u.)
OCNTH	HF	(1.38, 1.43)	6.912	354.573	23.638
	CIS		2.678	721.126	48.075
	DFT		2.034	423.125	28.208
	HF	(1.36, 1.45)	7.329	336.925	22.461
	CIS		2.961	670.732	44.715
	DFT		2.287	398.597	26.573
	HF	(1.34, 1.47)	7.720	323.860	21.590
	CIS		3.223	558.047	37.203
	DFT		2.523	379.663	25.310
	HF	(1.32, 1.49)	8.105	313.549	20.903
	CIS		3.479	466.914	31.127
	DFT		2.764	364.240	24.282
	HF	(1.40, 1.40)	6.441	381.876	25.458
	CIS		2.372	932.659	62.177
	DFT		1.770	458.860	30.590
	HF	(1.40, 1.41)	6.531	376.197	25.079
	CIS		2.432	897.229	59.815
	DFT		1.820	451.308	30.087
	HF	(1.42, 1.39)	9.252	692.525	43.282
	CIS		2.171	809.244	50.577
	DFT		4.012	699.454	43.715
	HF	(1.44, 1.37)	9.451	599.069	37.441
	CIS		2.418	784.286	49.017
	DFT		4.022	660.996	41.312
HF	(1.46, 1.35)	9.621	532.776	33.298	
CIS		2.667	778.854	48.678	
DFT		4.025	622.054	38.878	
HF	(1.48, 1.33)	9.770	484.451	30.278	
CIS		2.913	781.702	48.856	
DFT		4.031	584.432	36.527	
HF	(1.50, 1.31)	9.912	448.292	28.018	
CIS		3.181	778.176	48.636	
DFT		4.052	548.314	34.269	

Table 6.1 : Average polarizability per monomer of the molecules with the change of the oligomers for fully optimized geometry in SOS method.

Molecule	Oligomer	Approximate Average Polarizability (a.u.)	Average Polarizability (a.u.)	Approximate Average Polarizability per monomer (a.u.)	Average Polarizability per monomer (a.u.)
OTH	Monomer	5.72	48.829	5.72	48.829
	Dimer	31.18	106.49	15.59	53.245
	Tetramer	111.899	231.302	27.97	57.825
	Seximer	209.795	352.956	34.97	58.826
	Octamer	292.281	468.307	36.53	58.538
	Decamer	363.813	580.209	36.38	58.020
	12-mer	429.558		35.796	
	14-mer	494.647		35.33	
	16-mer	554.873		34.67	
OCY	Monomer	6.921	43.930	6.921	43.930
	Dimer	48.017	94.647	24.00	47.323
	Tetramer	180.502	217.194	45.12	54.298
	Seximer	334.474	335.816	55.74	55.969
	Octamer	461.292	443.809	57.66	55.476
	Decamer	614.678	546.613	61.46	54.661
	12-mer	730.067	647.531	60.83	53.960
OFV	Monomer	13.122	48.288	13.12	48.288
	Dimer	57.929	112.746	28.96	56.373
	Tetramer	212.087	260.03	53.02	65.007
	Seximer	385.013	397.04	64.16	66.173
	Octamer	542.375	524.161	67.79	65.520
OCNTH	Monomer	52.79	159.21	52.79	159.210
	Dimer	90.63	324.204	45.31	162.102
	Tetramer	179.788	657.298	44.94	164.324
	Seximer	152.487	656.598	25.41	109.433
OCNCY	Monomer	40.343	130.455	40.34	130.455
	Dimer	182.739	316.346	91.36	158.173
	Tetramer	440.04	616.917	110.01	154.229
	Seximer	584.977		97.49	
OCNFV	Monomer	48.75	152.727	48.75	152.727
	Dimer	184.94	367.79	92.47	183.895
	Tetramer	507.98	716.537	126.99	179.134
	Seximer	617.553		102.92	

Table 6.2 : Average polarizability per monomer of the molecules with the change of the oligomers for fully optimized geometry in CIS method.

Molecule	Oligomert	Polarizability (a.u.)						Average polarizability (a.u.)	Average Polarizability per monomer (a.u.)
		α_{xx}	α_{yy}	α_{zz}	α_{xy}	α_{yz}	α_{zx}		
OTH	Monomer	58.92	67.44	18.89	-0.001	0.000	0.000	48.419	48.419
	Dimer	238.20	110.17	34.90	3.527	0.000	0.000	127.755	63.87
	Tetramer	894.88	207.67	67.14	-16.11	-0.001	0.001	389.89	97.47
	Seximer	1778.05	305.39	99.38	10.95	0.001	0.000	727.60	121.27
	Octamer	2586.54	403.59	131.63	-11.99	-0.002	0.002	1040.584	130.07
	Decamer	3235.71	502.12	163.88	10.857	0.000	0.000	1300.57	130.06
OCY	Monomer	60.46	52.42	36.04	0.000	-3.359	0.000	49.637	49.637
	Dimer	262.17	98.20	50.12	-30.54	0.000	-0.003	136.826	68.413
	Tetramer	1122.79	188.80	83.54	-16.71	0.001	-0.014	465.045	116.26
	Seximer	2414.34	266.22	117.27	7.227	0.000	0.000	932.608	155.43
	Octamer	3648.39	344.56	151.06	-1.020	0.002	0.012	1381.133	172.64
	Decamer	4662.08	422.50	184.87	3.026	0.000	0.002	1756.484	175.64
	12-mer	5493.70	500.16	218.70	-6.584	-0.001	-0.013	2070.853	172.57
OFV	Monomer	82.084	71.34	32.77	0.000	0.005	0.002	62.061	62.061
	Dimer	231.75	173.15	41.95	18.68	0.000	0.000	148.948	74.47
	Tetramer	1337.03	314.15	67.34	220.38	0.000	0.000	572.839	143.209
	Seximer	2607.25	547.17	92.98	-608.65	0.000	0.000	1082.46	180.41
	Octamer	3834.08	711.12	118.69	855.58	0.000	0.000	1554.62	194.327
OCNTH	Monomer	228.75	225.86	46.76	-0.001	0.000	0.000	167.123	167.123
	Dimer	726.98	418.50	90.88	-19.83	0.000	0.000	412.118	206.059
	Tetramer	2515.64	1284.95	178.85	-62.28	0.000	0.000	1326.479	331.619
	Seximer	1737.19	1032.21	96.94	335.37	0.000	0.000	955.444	159.240
OCNCY	Monomer	271.11	209.09	60.53	0.000	0.000	0.000	180.242	180.242
	Dimer	1403.50	398.59	105.32	-34.60	-0.001	0.001	635.802	317.90
	Tetramer	2519.24	1277.41	194.94	844.38	0.000	0.000	1330.52	332.63
OCNFV	Monomer	317.39	298.70	53.17	0.000	0.000	0.000	223.082	223.082
	Dimer	1447.55	553.32	90.26	-77.82	0.000	0.000	697.042	348.52
	Tetramer	3861.17	1078.94	164.93	-467.36	0.000	0.000	1701.678	425.419

† here monomer, dimer, tetramer, seximer, octamer, decamer and 12-mer represent 1, 2, 4, 6, 8, 10 and 12 rings respectively.

Table 6.3 : Excitation energy and average polarizability per monomer of the molecules for fully optimized geometry in CIS method.

Molecule	Oligomer	Oscillator strength (arbitrary unit)	Excitation energy (eV)	Polarizability (a.u.)	Average Polarizability per monomer (a.u.)
OTH	Monomer	0.1418, 0.0000, 0.1442	5.5731, 6.5359, 6.7456	48.419	48.419
	Dimer	0.6262, 0.0000, 0.0000	4.1068, 6.1240, 6.2491	127.755	63.87
	Tetramer	1.5381, 0.0000, 0.0000	3.1903, 4.7260, 5.7430	389.89	97.47
	Seximer	2.317, 0.0000, 0.2692	2.9184, 4.0590, 4.8806	727.60	121.27
	Octamer	2.9660, 0.0000, 0.5040	2.8374, 3.7435, 4.3764	1040.584	130.07
	Decamer	3.5146, 0.0000, 0.8227	2.8204, 3.5812, 4.0784	1300.57	130.06
OCY	Monomer	0.2498, 0.0248, 0.0155	5.3693, 7.1494, 8.8741	49.637	49.637
	Dimer	1.4856, 0.0000, 0.0000	4.7866, 7.2640, 7.8401	136.826	68.413
	Tetramer	2.7516, 0.0000, 0.0000	3.3600, 5.1277, 5.3440	465.045	116.26
	Seximer	3.8956, 0.0000, 0.0000	2.9367, 4.3360, 4.7724	932.608	155.43
	Octamer	4.9054, 0.0000, 0.0000	2.8063, 3.9328, 4.6692	1381.133	172.64
	Decamer	5.8463, 0.0000, 1.3158	2.7739, 3.7133, 4.3258	1756.484	175.64
	12-mer	6.7059, 0.0000, 1.9093	2.7729, 3.5867, 4.0916	2070.853	172.57
OFV	Monomer	0.4642, 0.4504, 0.0012	6.4575, 8.2780, 8.5135	62.061	62.061
	Dimer	1.0054, 0.0000, 0.6724	4.0019, 6.5542, 6.5913	148.948	74.47
	Tetramer	2.5909, 0.0000, 0.1574	3.0503, 4.1467, 4.4497	572.839	143.209
	Seximer	3.7664, 0.0000, 0.3307	2.7404, 3.8030, 4.2392	1082.46	180.41
	Octamer	4.8292, 0.0000, 0.7290	2.6503, 3.5692, 4.0270	1554.62	194.327
OCNTH	Monomer	0.0420, 1.0458, 0.1505	1.9336, 4.3953, 5.0426	167.123	167.123
	Dimer	0.1431, 0.1921, 1.0543	1.7811, 2.8926, 4.4048	412.118	206.059
	Tetramer	0.8079, 0.0000, 0.3425	1.9879, 2.2798, 2.988	1326.479	331.619
	Seximer	0.3578, 1.4450, 0.0389	2.0123, 3.5510, 3.6141	955.444	159.240
OCNCY	Monomer	0.1551, 0.7844, 0.5090	3.5813, 5.4690, 5.6114	180.242	180.242
	Dimer	1.6571, 0.0000, 0.0000	2.5913, 3.8028, 4.3999	635.802	317.90
	Tetramer	2.0464, 1.5230, 1.4297	2.5688, 3.1560, 3.3030	1330.52	332.63
OCNFV	Monomer	0.0844, 0.6501, 0.6763	3.4738, 4.3194, 5.3092	223.082	223.082
	Dimer	1.3749, 0.0000, 0.0000	2.3461, 3.6457, 4.0257	697.042	348.52
	Tetramer	1.8309, 0.0000, 2.9899	2.3199, 2.9309, 2.9403	1701.678	425.419

Table 7.1: Average polarizability per monomer and excitation energy for dimer molecules for fully optimized geometry in three methods.

Molecule (dimer)	Method	Polarizability (a.u.)						Average polarizability (a.u.)	Average polarizability per monomer (a.u.)	Excitation energy (eV)
		α_{xx}	α_{yy}	α_{zz}	α_{xy}	α_{yz}	α_{xz}			
OTH	HF	110.72	148.13	34.58	1.161	0.000	0.000	97.81	48.90	11.912
	CIS	238.20	110.17	34.90	3.527	0.000	0.000	127.755	63.87	4.1068
	DFT	113.33	172.62	35.79	-2.903	0.000	0.000	107.25	53.62	5.826
OCY	HF	175.30	82.54	49.31	-2.782	0.000	0.004	102.38	51.19	10.533
	CIS	262.17	98.20	50.12	-30.54	0.000	-0.003	136.826	68.413	4.7866
	DFT	184.13	88.42	50.76	2.403	0.000	0.001	107.77	53.88	4.304
OFV	HF	135.68	196.58	41.47	22.794	0.000	0.000	124.57	62.28	12.139
	CIS	173.15	231.75	41.95	18.68	0.000	0.000	148.948	74.47	4.0019
	DFT	143.67	209.24	43.23	22.026	0.000	0.000	132.04	66.02	5.576
OCNTH	HF	401.05	518.04	91.15	20.334	0.000	0.000	336.74	168.37	7.3416
	CIS	418.50	726.98	90.88	-19.83	0.000	0.000	412.118	206.059	1.7811
	DFT	437.33	747.48	94.10	15.979	0.000	0.000	426.31	213.15	2.030
OCNCY	HF	696.85	330.30	105.46	44.454	-0.001	0.001	377.53	188.76	7.059
	CIS	1403.50	398.59	105.32	-34.60	-0.001	0.001	635.802	317.90	2.5913
	DFT	1005.18	370.44	109.04	-1.861	0.000	0.000	494.88	247.44	1.773
OCNFV	HF	420.34	789.66	90.44	9.414	0.000	0.000	433.48	216.74	9.425
	CIS	553.32	1447.55	90.26	-77.82	0.000	0.000	697.042	348.52	2.3461
	DFT	733.27	855.36	94.63	-300.35	0.000	0.000	561.09	280.54	3.472

Table 7.2: Description of the Gaussian keywords.

Keywords	Description
TRCIS	This keyword requests a calculation on excited states using single-excitation CI (CI-Singles).
OPT	This keyword requests that a geometry optimization be performed. The geometry will be adjusted until a stationary point on the potential surface is found.
FREQ	This keyword computes force constants and the resulting vibrational frequencies. When frequencies are done analytically, the polarizabilities are also computed automatically.
POLAR	This keyword requests that the dipole electric field polarizabilities (and hyperpolarizabilities, if possible) be computed.
POLAR=EnOnly	This keyword will produce both polarizabilities and hyperpolarizabilities.

